# VALLEY CURRENT IN GRAPHENE THROUGH ELECTRON-PHONON INTERACTION

A Thesis

by

ANKANG LIU

Submitted to the Graduate and Professional School of
Texas A&M University
in partial fulfillment of the requirements for the degree of

MASTER OF SCIENCE

| | |
|---|---|
| Chair of Committee, | Alexander Finkel'stein |
| Committee Members, | Artem Abanov |
| | Peter Kuchment |
| | Donald G. Naugle |
| | Valery L. Pokrovsky |
| Head of Department, | Grigory Rogachev |

December 2021

Major Subject: Physics

# ABSTRACT

Valleytronics which has a lot of advances in the information processing and conmunication requires the manipulation of the valley degree of freedom of the carriers. In this thesis, we discuss valley current, which is carried by quasiparticles in graphene. We show that the valley current arises owing to a peculiar term in the electron-phonon collision integral that mixes the scalar and vector gauge-field-like vertices in the electron-phonon interaction. This mixing makes collisions of phonons with electrons sensitive to their chirality, which is opposite in two valleys. As a result of collisions with phonons, electrons of the different valleys deviate in opposite directions. The valley-dependent deviation of the quasiparticle current does not request for breaking the spatial inversion symmetry. The effect exists both in pristine graphene or bilayer graphene samples, and it increases with temperature owing to a higher rate of collisions with phonons at higher temperatures. The valley current carried by quasiparticles could be detected by measuring the electric current using a nonlocal transformer of a suitable design. This could open up another unexplored possibility in the area of valleytronics.

ACKNOWLEDGMENTS

I would like to express my deep gratitude and great thanks to my advisor, Dr. Alexander M. Finkel'stein, for his constant guidance, great patience and much helpful advice.

CONTRIBUTORS AND FUNDING SOURCES

## Contributors

This work was supported by a thesis committee consisting of Professor Alexander Finkel'stein, Artem Abanov, Donald Naugle, and Valery Pokrovsky of the Department of Physics & Astronomy and Professor Peter Kuchement of the Department of Mathematics.

All work conducted for the thesis was completed by the student under the supervision of Professor Alexander Finkel'stein.

## Funding Sources

Graduate study was supported by a graduate teaching/research assistantship from the Department of Physics & Astronomy of Texas A&M University and research grants from the Veronika A. Rabl Physics Discretionary Fund and the Benoziyo Endowment Fund for the Advancement of Science.

# LIST OF SYMBOLS

| | |
|---|---|
| $K/K'$ | Two letters used to denote two non-degenerated valleys. |
| $\Psi_{\boldsymbol{p}}$ | The fermion operator, which is a spinor defined in A/B-sublattice space. |
| $H_{\boldsymbol{p}}$ | A 2×2 matrix which describes the tight binding model of free electron Hamiltonian of graphene in A/B-sublattice space. |
| $M_{\boldsymbol{q}}$ | A 2×2 matrix which describes electron-phonon interaction of graphene in A/B-sublattice space. |
| $A_{\boldsymbol{q}}$ | The bosonic field, $A_{\boldsymbol{q}} = b_{\boldsymbol{q}} + b^{\dagger}_{-\boldsymbol{q}}$, which describes the annihilation and creation of the longitudinal phonons. |
| $v_F$ | The Fermi velocity. |
| $\epsilon_F$ | The Fermi energy. |
| $\sigma_{x/y}$ | Standard Pauli matrices defined in A/B-sublattice space. |
| $g_{1/2}$ | $g_1$ is the deformation potential, while $g_2$ is the vector potential. |
| $\theta_{\boldsymbol{q}}$ | The angle between the phonon's momentum $\boldsymbol{q}$ and the $x$ direction. |
| $\eta$ | The angle of the $x$ direction measured from the zigzag direction if the honeycomb lattice. |
| $v_s$ | The speed of sound in graphene. |
| $\xi_{\boldsymbol{p}}$ | $\xi_{\boldsymbol{p}} = v_F p - \epsilon_F$ is the energy measured from the Fermi surface. |
| $G^{K/R/A}$ | The Keldysh, retarded and advanced component of the Green's function for electrons, which are 2×2 matrices for graphene. |
| $g^{K/R/A}$ | The Keldysh, retarded and advanced component of the quasi-classical Green's function (i.e., the $\xi$-integrated Green's function) for electrons, which are 2×2 matrices for graphene. |

| | |
|---|---|
| $\boldsymbol{n_p}$ | $\boldsymbol{n_p} = \boldsymbol{p}/p$ is a unit vector describes the direction of electron's momentum $\boldsymbol{p}$. |
| $n$ | The distribution function of phonons. |
| $\nu_0$ | $\nu_0 = p_F/2\pi v_F$ is the density of state for the electron per valley and per spin. |
| $\boldsymbol{d}$ | $\boldsymbol{d} = (cos2\theta_{\boldsymbol{q}}, -sin2\theta_{\boldsymbol{q}})$ is a unit vector associated with the vector gauge-field-like vertex. |
| $f$ | The distribution function of electrons. |
| $p_F$ | The Fermi momentum. |
| $\hat{\boldsymbol{v}}$ | The velocity operator $\partial_{\boldsymbol{p}} H_{\boldsymbol{p}} = v_F(\sigma_x, \sigma_y)$ for graphene, which is a $2\times2$ matrix vector. |
| $t_i$ | The hopping energy between A- and B-sublattice along the direction $\boldsymbol{\tau}_i$. |
| $\boldsymbol{u}$ | The lattice displacement. |
| $u_{ij}$ | The dimensionless strain tensor. |
| $\Phi_{\boldsymbol{E}}$ | The electric potential energy. |
| $\varphi$ | The quantity which parameterizes the small deviation of the electronic distribution from its equilibrium; it has the dimension of energy. All other quantities denoted with $\varphi$ such as $\varphi_1^{K/K'}$, $\tilde{\varphi}_{\mathcal{B}}$, and $\varphi_{\mathcal{C}}$, have also the dimension of energy. |
| $\tau$ | The relaxation time for the electronic distribution in the valley-independent scatterings. |
| $A_E$ | The coefficient in front of the Drude-kind solution, which has the dimension of energy. |
| $l$ | $l \equiv v_F\tau$ is the mean free path length. |
| $B_{ph}^{(2/4)}$ | The coefficients in front of the second and forth harmonic solutions, respectively, which have the dimension of energy. |
| $\Gamma_{e-ph}^{(2/4)}$ | The electron-phonon collision rates which generate the second and forth harmonics, respectively. |
| $T_{BG}$ | $T_{BG} \equiv 2v_s p_F$ is the Bloch-Grüneisen temperature, which is $\approx 57\sqrt{\tilde{n}}\ K$ in graphene for longitudinal phonons. |

| | |
|---|---|
| $\tilde{n}$ | The dimensionless concentration when the electron density is measured in units $10^{12}\ cm^{-2}$. |
| $\varphi_1^{K/K'}$ | The valley-dependent deviations of the electronic distribution caused by the valley-dependent electron-phonon scattering. |
| $\mathcal{A}$, $\mathcal{B}$, $\mathcal{C}$, $\tilde{\mathcal{C}}$, $\mathcal{D}$, and $\tilde{\mathcal{D}}$ | The letters used to denote the different regions in our designed geometry. |
| $\mu^{K/K'}$ | The valley-dependent chemical potential. |
| $\boldsymbol{j}_v$ | $\boldsymbol{j}_v \equiv \boldsymbol{j}^K - \boldsymbol{j}^{K'}$ is the valley current density. |
| $\sigma_0$ | The Drude conductivity for graphene per valley and per spin. |
| $\tilde{\varphi}_{\mathcal{B}}$ | The valley-independent electronic distribution in the branch $\mathcal{B}$. |
| $D_{ph}^{(2)}$ | The coefficient in front of the valley-independent distribution $\tilde{\varphi}_{\mathcal{B}}$, which has the dimension of energy. |
| $\varphi_{\mathcal{C}}$ | The Drude form distribution in the branch $\mathcal{C}$. |
| $E_{\mathcal{C}/\mathcal{D}}$ | The effective electric filed associated with the Drude form solutions in the branch $\mathcal{C}$ and $\mathcal{D}$, respectively. |
| $\sigma_q$ | $\sigma_q \equiv e^2/h$ with $h$ to be the Planck constant is the quantum conductance; $\sigma_q \approx (25.8\ k\Omega)^{-1}$. |
| $l_v$ | The intervalley scattering length. |
| $w_{\mathcal{C}/\mathcal{D}}$ | The widths of the branch $\mathcal{C}$ and $\mathcal{D}$, respectively. |
| $I_{\mathcal{C}/\mathcal{D}}$ | The currents measured within the branch $\mathcal{C}$ and $\mathcal{D}$, respectively. |
| $\Sigma^{K/R/A}$ | The Keldysh, retarded and advanced component of the electronic self-energy, which are $2\times2$ matrices for graphene. |
| $D^{K/R/A}$ | The Keldysh, retarded and advanced component of the Green's function for phonons, which are scalar quantities. |
| $h$ | The standard notation for the distribution function for fermions which connects the Keldysh component of the Green's function to the retarded and advanced components. |

| | |
|---|---|
| $N$ | The standard notation for the distribution function for bosons which connects the Keldysh component of the Green's function to the retarded and advanced components. |

TABLE OF CONTENTS

Page

# 1. INTRODUCTION*

Information technology based on the conventional electronic devices requires the ability to manipulate the electric charge of the carriers. However, there are a lot of disadvantages when operating the electric charge. For example, a flow of electric charge generates the Joule heating. To reduce the power consumption, there is an emerging field called spintronics which exploits another degree of freedom, the spin of the carriers. In this way, one could transfer the data which is encoded in the spin current to avoid the Joule heating, and thus increase the energy efficiency of the devices. Nevertheless, spintronics is limited by the spin diffusion length. The magnetic impurities in the sample would reduce the spin diffusion length significantly, therefore limit the applicability of spintronics devices. On the other side, the electrons in 2D materials such like graphene and transition metal dichalcogenides (TMDs) acquire the valley degree of freedom [1]. Two valleys in these materials are separated by large momentum $p \sim \frac{1}{a}$ in momentum space with $a$ to be the lattice constant. As a result, the valley diffusion length is considerably long in these systems. Utilizing this new degree of freedom leads to a new possibility to process information. In this thesis, we discuss a possible way to generate and detect the valley current in graphene through electron-phonon (*el-ph*) interaction. The thesis is written based on my published work on Phys. Rev. B [2].

Graphene [3, 4] is a two-dimensional (2D) sheet of carbon atoms with a honeycomb lattice. One characteristic of the honeycomb lattice is its band structure which, in the case of pristine graphene, has Dirac cones located at the corners of the first Brillouin zone [5]. The Dirac cones at two nonequivalent points of the corners are called the $K$ and $K'$ valleys, respectively. Recently, physicists are more and more interested in the valley-related physics, which forms a new subject called valleytronics [1]. The control of the valley degrees of freedom could be potentially used for quantum computations and communications.

*Part of this chapter is reprinted with permission from "Valley current in graphene through electron-phonon interaction" by Ankang Liu and Alexander M. Finkel'stein, 2020. Phys. Rev. B, 101, 241401, Copyright 2020 by American Physical Society.

Systems with honeycomb lattices possess a nonzero Berry curvature, opposite in the two valleys, if the band gap is opened when spatial inversion symmetry is broken [6, 7, 8]. The nonzero Berry curvature may reveal itself via the valley Hall effect which is reminiscent of the spin Hall effect [9]. Remarkably, some experimental groups have already confirmed that this valley dependent effect could be measured through a nonlocal transport in graphene superlattices [10] or in a dual-gated bilayer graphene sample [11, 12]. Because of an extremely low intervalley scattering rate, the valley current could be detected at distances exceeding 1 $\mu m$.

Still, transport studies which relied on the Berry curvature physics [7] needed a system with broken inversion symmetry and low temperatures. By contrast, in this thesis we discuss the possibility of working with a valley current transported by quasiparticles at high temperatures in pristine graphene, both single and double layered. For this purpose, we identified the valley-dependent process in the *el-ph* scattering, using the fact that one of the amplitudes of the *el-ph* interaction is sensitive to the chirality of the quasiparticles, which is opposite in the two valleys. By solving the quantum kinetic equation for the *el-ph* scattering in the presence of an external electric field, we demonstrate that the distribution of the quasiparticles contains a term with a quadruple angular dependence, different for the two valleys. In short, current carriers passing through a population of phonons are turned by them in different directions for the two valleys. This opens an opportunity for controlling the valley currents using samples with a designed geometry. The whole effect is owing to transitions between the two sublattices of the honeycomb lattice caused by *el-ph* scattering. The discussed mechanism holds for any honeycomb lattice system.

The thesis is organized as follows. First, we consider the single layered graphene. In Chapter 2 we derive a quantum kinetic equation with the *el-ph* collision integral. Both the scalar and vector gauge-field-like vertices in the *el-ph* interaction were included. Then, we discuss the transformation of the obtained quantum kinetic equation from the $K$ to $K'$ valley in Chapter 3. From this we observe that a mixture of the scalar and vector gauge-field-like vertices generates a term in the *el-ph* collision integral, which is different in two valleys. In Chapter 4, the solution of the quantum kinetic equation under an external electric field is given. Here we notice that there exists a val-

ley dependent distribution for electrons, which exhibits a non-trivial angular dependence. Next, in Chapter 5, show how to exploit the angular dependent distribution for the valley-transport measurements. We design a certain geometry of the sample, and show how a valley current transported by the quasi-particle excitations could be experimentally generated and detected. Finally, the discussion and conclusion are given in Chapter 6. The comprehensive derivation of the quantum kinetic equation and the *el-ph* collision integral that we used in the main text, some supporting arguments and discussions, and details of the solution could be found in the Appendices. The consideration of the double layered graphene is quite similar to that of the single layer. We leave the discussion on the double layered graphene to Appendix E.

## 2. QUANTUM KINETIC EQUATION*

In order to study the transport, we derive the quantum kinetic equation in the case of a single-layer graphene. (For bilayer graphene, see Appendix E.) The free-electron and the *el-ph* interaction terms in the Hamiltonian are $H_e = \sum_{\boldsymbol{p}} \Psi^\dagger_{\boldsymbol{p}} H_{\boldsymbol{p}} \Psi_{\boldsymbol{p}}$ and $H_{e-ph} = \sum_{\boldsymbol{p},\boldsymbol{q}} \Psi^\dagger_{\boldsymbol{p}+\boldsymbol{q}} M_{\boldsymbol{q}} \Psi_{\boldsymbol{p}} A_{\boldsymbol{q}}$, respectively. Here, the fermion operator $\Psi_{\boldsymbol{p}}$ is a spinor defined in the sublattice space, and the bosonic field $A_{\boldsymbol{q}} = b_{\boldsymbol{q}} + b^\dagger_{-\boldsymbol{q}}$ describes the annihilation and creation of the longitudinal phonons. In this research, we consider the interaction with the longitudinal phonons, because only they provide electrons with a valley-dependent dynamics, which we are interested in.

We first concentrate on one of the valleys. The kinetic term for electrons in the $K$ valley, $H^K_{\boldsymbol{p}} = v_F \boldsymbol{\sigma} \cdot \boldsymbol{p} - \epsilon_F \mathbb{1}_{2\times 2}$, is obtained from the standard tight-binding model for the honeycomb lattice [3, 4, 5]. Here, $\epsilon_F$ is the Fermi energy, and components of the matrix vector $\boldsymbol{\sigma} = (\sigma_x, \sigma_y)$ are the standard Pauli matrices. We assume that the system is not too close to the neutral point, but at the level of the current carrier concentrations typical for metallic graphene. For the longitudinal acoustic phonons, the matrix elements of the *el-ph* interaction are described by a $2 \times 2$ matrix [13, 14, 15],

$$M^K_{\boldsymbol{q}} = |\boldsymbol{q}| \sqrt{\frac{1}{2\rho\omega_{\boldsymbol{q}}}} \begin{pmatrix} g_1 & g_2 e^{i(2\theta_{\boldsymbol{q}}+3\eta)} \\ g_2 e^{-i(2\theta_{\boldsymbol{q}}+3\eta)} & g_1 \end{pmatrix}. \tag{2.1}$$

We are mostly interested in the details of the off-diagonal elements of this matrix. Here, $\theta_{\boldsymbol{q}}$ is the angle between the phonon's momentum $\boldsymbol{q}$ and the $x$ direction, while $\eta$ is the angle of the $x$ direction measured from the zigzag direction of the honeycomb lattice. The combination in front of the parentheses is standard for the *el-ph* interaction with acoustic phonons: $\rho$ is the mass density of the graphene sample, and $\omega_{\boldsymbol{q}} = v_s|\boldsymbol{q}|$ is the phonon frequency for the longitudinal acoustic mode with $v_s \ll v_F$.

*Reprinted with permission from "Valley current in graphene through electron-phonon interaction" by Ankang Liu and Alexander M. Finkel'stein, 2020. Phys. Rev. B, 101, 241401, Copyright 2020 by American Physical Society.

In matrix $M_{\boldsymbol{q}}$, the diagonal coupling constant $g_1$ comes from the deformation potential (DP), and before screening has a bare value of 20-30 eV [14]. The magnitude of $g_2$ has been estimated to be 1.5 eV. The term affiliated with $g_2$ reveals some similarities with the vector potential (VP) for the electromagnetic field [14, 15, 16, 17].

To obtain the *el-ph* collision integral in the quantum kinetic equation, we consider the self-energy diagram presented in Fig. 2.1. In the derivation of the quantum kinetic equation we apply

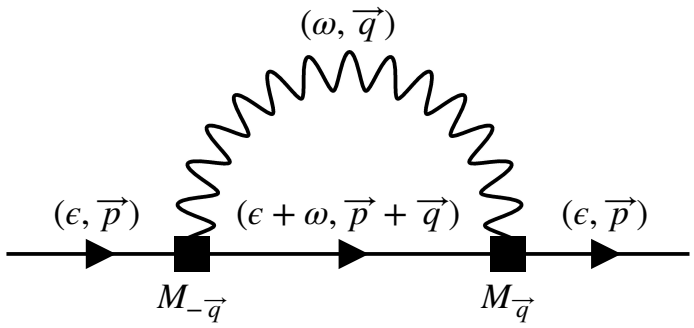


Figure 2.1: The electronic self-energy due to the *el-ph* interaction. The solid line represents the electron propagator while the wavy line means the phonon propagator. The black square here is the full *el-ph* vertex, which contains both the scalar and vector gauge-field-like part of the vertex.

the quasiclassical approximation [18, 19, 20]. We rely on the fact that for the *el-ph* interaction the self-energy has a weak dependence on $\xi_{\boldsymbol{p}} = v_F p - \epsilon_F$. In the quasiclassical approximation, the electron momentum $\boldsymbol{p}$ is placed on the Fermi surface. This could be achieved by integrating the Green's functions with respect to $\xi_{\boldsymbol{p}}$: $g^{K/R/A} = \frac{i}{\pi} \int d\xi_{\boldsymbol{p}} G^{K/R/A}$. The remaining dependence on an electron direction is described by a unit vector $\boldsymbol{n_p} = \boldsymbol{p}/p$. The reason to use quasiclassics is that we are interested in the effects related to the angular dependencies.

The *el-ph* collision integral $I_{e-ph}(f, n)$ has to be written in terms of $f$, the quasiclassical distribution function of electrons, and the distribution function of phonons $n$. For our purposes it will be enough to assume that phonons are under thermal equilibrium, i.e., $n = n_0(\omega) = (e^{\omega/T} - 1)^{-1}$. The *el-ph* collision integral for electrons in the $K$ valley contains (among others) the following

specific term [Appendix A],

$$I^{v}_{e-ph}(f,n) = 2\pi\nu_0 \int d\epsilon' \int \frac{d\theta_{\boldsymbol{p}'}}{2\pi} \alpha(q) g_1 g_2 (\boldsymbol{n_p} + \boldsymbol{n_{p'}}) \cdot \boldsymbol{d} \\ \times \big[ f'(1-f)(1+n) - f(1-f')n \big] (\delta_+ - \delta_-). \tag{2.2}$$

Here, $\nu_0 = p_F/2\pi v_F$ is the density of state for the electron per valley and per spin, $\alpha(q) = q^2/2\rho\omega_{\boldsymbol{q}}$, and $\boldsymbol{d} = (cos2\theta_{\boldsymbol{q}}, -sin2\theta_{\boldsymbol{q}})$ is a unit vector associated with the vector gauge-field-like vertex. Without loss of generality, we take here $\eta = 0$ assuming that our $x$ direction is along the so-called zigzag lattice direction. We also use short notations here: $f = f(\epsilon, \boldsymbol{n_p})$, $f' = f(\epsilon', \boldsymbol{n_{p'}})$, $n = n_0(\epsilon' - \epsilon)$, and $\boldsymbol{q} = p_F(\boldsymbol{n_{p'}} - \boldsymbol{n_p})$. Energy conservation in the collision integral is controlled by $\delta_\pm = \delta(\epsilon' - \epsilon \mp v_s p_F |\boldsymbol{n_{p'}} - \boldsymbol{n_p}|)$.

## 3. TRANSFORMATION FROM $K$ TO $K'$ VALLEY*

For electrons in the $K'$ valley, the kinetic term $H_{\boldsymbol{p}}^{K'} = v_F(-p_x\sigma_x + p_y\sigma_y) - \epsilon_F \mathbb{1}_{2\times 2}$ [3, 4, 5]. Next, the *el-ph* interaction is given by the matrix $M_{\boldsymbol{q}}^{K'}$, which is connected to the $M_{\boldsymbol{q}}^{K}$ through the relation $M_{\boldsymbol{q}}^{K'} = \left(M_{-\boldsymbol{q}}^{K}\right)^*$ [14, 15]. One may observe that the transformation from the $K$ to $K'$ valley could be achieved by using the following substitutions (again, we set here $\eta = 0$):
(i) $\hat{\boldsymbol{v}}^K = v_F(\sigma_x, \sigma_y) \to \hat{\boldsymbol{v}}^{K'} = v_F(-\sigma_x, \sigma_y)$; (ii) $\boldsymbol{n}_{\boldsymbol{p}}^K = (cos\theta_{\boldsymbol{p}}, sin\theta_{\boldsymbol{p}}) \to \boldsymbol{n}_{\boldsymbol{p}}^{K'} = (-cos\theta_{\boldsymbol{p}}, sin\theta_{\boldsymbol{p}})$; and (iii) $\boldsymbol{d}^K = (cos2\theta_{\boldsymbol{q}}, -sin2\theta_{\boldsymbol{q}}) \to \boldsymbol{d}^{K'} = (cos2\theta_{\boldsymbol{q}}, sin2\theta_{\boldsymbol{q}})$.

With the use of these transformations, one could check that the collision term in the quantum kinetic equation remains unchanged for the $K'$ valley, except that the $g_1 g_2$ term presented by Eq. (2.2) acquires an opposite sign. We ascribe the peculiarity of this valley-dependent term to the origin of the vector gauge-field-like vertex (VP). Indeed, the $g_2$ term, as the off-diagonal part of the *el-ph* vertex, comes from the intersublattice hopping mediated by the lattice vibrations. Consequently, this term is sensitive to the direction of the quasimomentum as well as to the chirality of electrons and, hence, is different in two valleys. On the contrary, the scalar $g_1$ term is the on-site energy, which is valley independent. Therefore, only the mixture of $g_1$ and $g_2$ terms would produce a valley-contrasting term $(\boldsymbol{n_p} \cdot \boldsymbol{d})^{K/K'}$ in the collision integral that leads to a valley-dependent dynamics.

In this paragraph, we present a detailed way to see how the free electron and *el-ph* interaction Hamiltonian are transformed from one valley to another. To understand how the difference in two valleys arises, one needs to look at the lattice structure of graphene. As shown in FIG. 3.1, each A atom has three nearest neighbor B atoms, and vise versa. Hence, the off-diagonal elements of the tight-binding Hamiltonian are $\langle\psi_{A,\boldsymbol{k}}|\,\hat{\mathcal{H}}\,|\psi_{B,\boldsymbol{k}}\rangle = \langle\psi_{B,\boldsymbol{k}}|\,\hat{\mathcal{H}}\,|\psi_{A,\boldsymbol{k}}\rangle^* = \sum_{i=1}^{3} t_i e^{i\boldsymbol{k}\cdot\boldsymbol{\tau}_i}$, with $|\psi_{A,\boldsymbol{k}}\rangle$ and $|\psi_{B,\boldsymbol{k}}\rangle$ to be the Bloch wave functions for A and B sublattices. Here, $\boldsymbol{\tau}_1 = a(0, \frac{\sqrt{3}}{3})$, $\boldsymbol{\tau}_2 = a(-\frac{1}{2}, -\frac{\sqrt{3}}{6})$, and $\boldsymbol{\tau}_3 = a(\frac{1}{2}, -\frac{\sqrt{3}}{6})$; for simplicity, we took $\eta = 0$ in the definition of $x, y$ axis.

*Reprinted with permission from "Valley current in graphene through electron-phonon interaction" by Ankang Liu and Alexander M. Finkel'stein, 2020. Phys. Rev. B, 101, 241401, Copyright 2020 by American Physical Society.

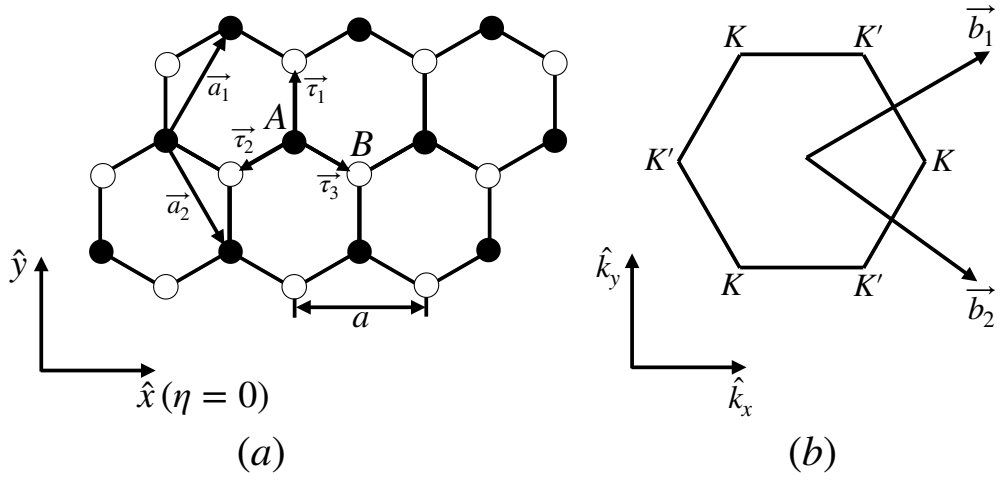


Figure 3.1: (a) Lattice of graphene with two sublattices A and B indicated by black and white circles, respectively. The two primitive vectors are $\vec{a_1} = a(\frac{1}{2}, \frac{\sqrt{3}}{2})$, and $\vec{a_2} = a(\frac{1}{2}, -\frac{\sqrt{3}}{2})$ ($a$ is the lattice constant). (b) The first Brillouin zone of graphene which contains two nonequivalent points $K$ and $K'$. The two reciprocal primitive vectors are $\vec{b_1} = \frac{2\pi}{a}(1, \frac{\sqrt{3}}{3})$ and $\vec{b_2} = \frac{2\pi}{a}(1, -\frac{\sqrt{3}}{3})$.

Matrix elements describing hopping along the directions $\boldsymbol{\tau}_i$ consist of two terms, $t_i = t_0 + \delta t_i$. The static $t_0$ is the same for all three directions, and it determines the dispersion of free electrons. Indeed, for electrons with momenta around $K/K'$ points, i.e., when $\boldsymbol{k} = (\pm\frac{4\pi}{3a}, 0) + \boldsymbol{p}$, the lowest order expansion in $\boldsymbol{p}$ of the $t_0$-hopping from $A$ to $B$ sublattice yields $v_F(\pm p_x - ip_y)$, with $v_F = -\frac{\sqrt{3}a}{2}t_0$. This is consistent with $H_{\boldsymbol{p}}^{K/K'}$. Furthermore, the terms $\delta t_i$ originate as a result of the bond length changes caused by the lattice displacements $\boldsymbol{u}$; this yields $\delta t_i \propto \frac{1}{a}(\frac{\partial t_0}{\partial a})\boldsymbol{\tau}_i \cdot [(\boldsymbol{\tau}_i \cdot \nabla_{\boldsymbol{r}})\boldsymbol{u}]$ [14]. Then, for $\sum_{i=1}^{3} \delta t_i e^{i\boldsymbol{k}\cdot\boldsymbol{\tau}_i}$ calculated at the points $K/K'$ one gets two terms that are $\propto -\frac{a}{4}(\frac{\partial t_0}{\partial a})[(u_{xx} - u_{yy}) \pm 2iu_{xy}]$, where $u_{ij}$ is the dimensionless strain tensor. Next, for the longitudinal phonon mode, the displacement $\boldsymbol{u} \propto \sum_{\boldsymbol{q}} \sqrt{\frac{1}{2\rho\omega_{\boldsymbol{q}}}}(i\hat{\boldsymbol{q}})(b_{\boldsymbol{q}} + b_{-\boldsymbol{q}}^{\dagger})e^{i\boldsymbol{q}\cdot\boldsymbol{r}}$, that leads to $u_{ij} \propto \sum_{\boldsymbol{q}} \sqrt{\frac{1}{2\rho\omega_{\boldsymbol{q}}}}|\boldsymbol{q}|\hat{q}_i\hat{q}_j(b_{\boldsymbol{q}} + b_{-\boldsymbol{q}}^{\dagger})e^{i\boldsymbol{q}\cdot\boldsymbol{r}}$. After a straightforward substitution into the matrix elements of the $\delta t_i$-hopping terms, one recovers the phase factors $e^{\pm i2\theta_{\boldsymbol{q}}}$ in the off-diagonal elements of the matrices $M_{\boldsymbol{q}}^{K/K'}$.

As a result, one could easily check that the valley-dependent Hamiltonians of free electrons as well as the *el-ph* interaction in the two valleys obey the mutual transformations presented in

the main text. This, eventually, leads to a non-trivial valley-contrasting term in the *el-ph* collision integral. Note that the quantum kinetic equation Eq. (A.15) as well as the electric current density Eq. (A.17), which are of general character, are unaltered under these transformations.

## 4. VALLEY-DEPENDENT DYNAMICS UNDER AN EXTERNAL ELECTRIC FIELD*

In the presence of an electric field, $\boldsymbol{E} = -\boldsymbol{\nabla}\Phi_{\boldsymbol{E}}$, we parametrize $\delta f$, a small deviation of the electron distribution function from the local equilibrium $f_0 = (e^{(\epsilon - e\Phi_{\boldsymbol{E}})/T}+1)^{-1}$, as $\delta f = (-\frac{\partial f_0}{\partial \epsilon})\varphi$ [21]. In the linear response regime, we have to solve the equation for the steady solution $\varphi$,

$$v_F e\boldsymbol{E}\cdot\boldsymbol{n_p}\frac{\partial f_0}{\partial \epsilon} = I_0(\varphi) + [I^v_{e-ph}]^{K/K'}(\varphi). \tag{4.1}$$

Here $I_0(\varphi) = \frac{\partial f_0}{\partial \epsilon}\varphi/\tau$ is a valley-independent collision term written in the relaxation time approximation. $I_0(\varphi)$ has been introduced to account for the valley-independent scatterings which determine the conventional transport properties of the system, e.g., the electron-impurity scattering. For simplicity, we will assume here that the valley-independent scattering is mostly of a short-ranged character. i.e., the relaxation time $\tau$ is same for harmonics of different orders [22]. The other term in Eq. (4.1) describes the valley-dependent part of the collision integrals [*cf.* Eq. (2.2)],

$$\begin{aligned}[I^v_{e-ph}]^{K/K'}(\varphi) = \pm 2\pi\nu_0 \int d\epsilon' \int \frac{d\theta_{\boldsymbol{p}'}}{2\pi}\alpha(q)[g_1 g_2(\boldsymbol{n_p}+\boldsymbol{n_{p'}})\cdot\boldsymbol{d}](\frac{\partial n_0}{\partial\omega})\Big|_{\omega=\epsilon'-\epsilon} \\ \times (f_0' - f_0)(\varphi'-\varphi)(\delta_+ - \delta_-).\end{aligned} \tag{4.2}$$

Here, $\pm$ refers to the $K/K'$ valleys.

One can show that Eq. (4.1) can be solved perturbatively [Appendix C], assuming $\varphi$ to be $\varphi \simeq \varphi_0 + \varphi_1^{K/K'}$ with $\varphi_0 \gg \varphi_1^{K/K'}$. Then, the functions $\varphi_0$ and $\varphi_1^{K/K'}$ have to satisfy two iteration

*Reprinted with permission from "Valley current in graphene through electron-phonon interaction" by Ankang Liu and Alexander M. Finkel'stein, 2020. Phys. Rev. B, 101, 241401, Copyright 2020 by American Physical Society.

equations,

$$v_F eE\frac{\partial f_0}{\partial \epsilon}cos\theta_{\boldsymbol{p}} = I_0(\varphi_0),$$
$$I_0(\varphi_1^{K/K'}) + [I^v_{e-ph}]^{K/K'}(\varphi_0) = 0. \tag{4.3}$$

We seek for a Drude-kind solution $\varphi_0 = A_E cos\theta_{\boldsymbol{p}}$ with $A_E = eEl$, where the mean free path length $l \equiv v_F\tau$. Then, the term mixing the two vertices in the *el-ph* interaction generates a nontrivial angular dependence in the distribution function,

$$\varphi_1^{K/K'} = \mp[B^{(2)}_{ph}cos(2\theta_{\boldsymbol{p}}) + B^{(4)}_{ph}cos(4\theta_{\boldsymbol{p}})], \tag{4.4}$$

with $B^{(2/4)}_{ph} = (\Gamma^{(2/4)}_{e-ph}\tau)A_E$. [Here, and in Eq. (4.3), we took for simplicity $\boldsymbol{E} = E(1,0)$ to be along the zigzag direction for which $\eta = 0$.] It turned out that the fourth harmonic (for numerical reasons) yields only a negligible correction to the effect that we are interested in. We therefore omit the fourth harmonic in the consideration below. The appearance of the quadruple valley-dependent term in the distribution function of the current-carrying state is the central observation of this research work.

To utilize the valley-dependent angular distribution generated by the *el-ph* scattering, we will be interested in relatively high temperatures, e.g., room temperature and above, when $T \gg T_{BG}$; $T_{BG} \equiv 2v_s p_F$ is the Bloch-Grüneisen temperature. (For the sake of convenience, we introduce now a dimensionless concentration $\tilde{n}$, so that the electron concentration $n = \tilde{n} \times 10^{12}\ cm^{-2}$. Then, the Bloch-Grüneisen temperature depends on $\tilde{n}$ as $T_{BG} \approx 57 \times \sqrt{\tilde{n}}\ K$.) For temperatures much exceeding $T_{BG}$, the rate $\Gamma^{(2)}_{e-ph}$ is estimated to be [Appendix C]

$$\Gamma^{(2)}_{e-ph} \simeq 3 \times 10^{-3}\tilde{n}\left(\frac{T}{T_{BG}(\tilde{n})}\right)\ ps^{-1}. \tag{4.5}$$

## 5. GENERATION AND DETECTION OF THE VALLEY CURRENT*

We are ready to show how the valley current arises as a result of the valley-dependent $\varphi_1^{K/K'}$, and suggest a scheme of detecting a nonlocal signal. Let us consider the geometry presented in Fig. 5.1. In region $\mathcal{A}$, the electric current flows along the $x$ direction. As we have shown,

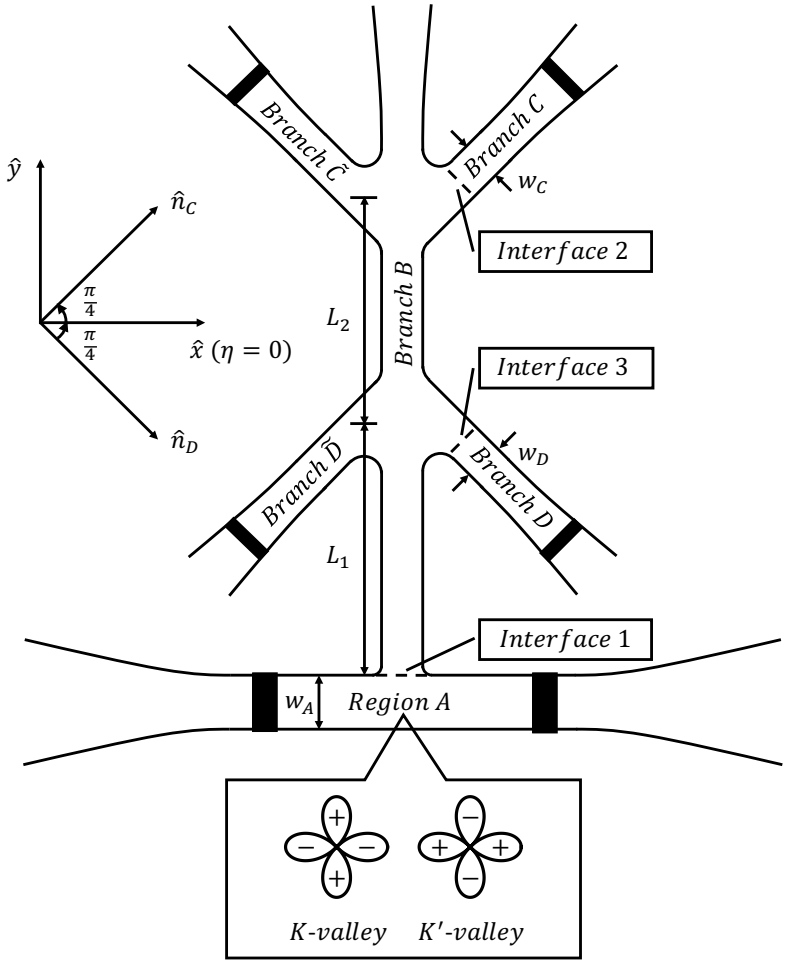


Figure 5.1: The geometry of a graphene sample suggested for the generation and detection of the valley current. At the bottom, the valley-dependent quadruple distributions caused by the *el-ph* scattering inside the region $\mathcal{A}$ are shown, where the $\pm$ sign means the excess and deficit of the distributed carriers with certain momentum directions.

*Reprinted with permission from "Valley current in graphene through electron-phonon interaction" by Ankang Liu and Alexander M. Finkel'stein, 2020. Phys. Rev. B, 101, 241401, Copyright 2020 by American Physical Society.

the distribution function contains the valley-dependent quadruple term $\varphi_1^{K/K'}$. In a sample with the discussed geometry, $\varphi_1^{K/K'}$ leads to a valley current that propagates along branch $\mathcal{B}$. Indeed, let us consider interface 1 (a conditional boundary between regions $\mathcal{A}$ and $\mathcal{B}$). The carriers with $\pi \geq \theta_{\boldsymbol{p}} \geq 0$ leave region $\mathcal{A}$, pass through the interface, and enter region $\mathcal{B}$. Consequently, the distribution $\varphi_1^K$ provides a nonzero upward flux through interface 1 and, eventually, an upward flow of the $K$-valley carriers. The carriers in the $K'$ valley would react oppositely. Finally, there will be a valley current along branch $\mathcal{B}$. This is similar to the injection of the spin current in spintronic devices.

The distribution functions that introduce the fluxes of the $K$- and $K'$-valley carriers inside branch $\mathcal{B}$, after a few scattering events [23], acquire the Drude-like form directed oppositely for two valleys. In other words, at a distance $l_{eq} \gtrsim l$, but much less than the intervalley scattering length $l_v$, one can introduce the valley-dependent chemical potentials $\mu^{K/K'} = \bar{\mu} + \delta\mu^{K/K'}(y)$, and apply the diffusion approximation for the flux-carrying particles (an example of conversion into the Drude-like form of the flux injected into disordered bridge can be found in Ref. [24]). Note that because of the electroneutrality, $\delta\mu^K = -\delta\mu^{K'}$. In order to maintain a stationary valley current flow deep inside the branch $\mathcal{B}$, $\delta\mu^{K/K'}$ would have a linear spatial dependence, i.e., $\boldsymbol{\nabla}(\delta\mu^{K/K'}) = \mp l^{-1} C_{\mathcal{B}} \hat{\boldsymbol{y}}$. The distribution functions $\varphi_{\mathcal{B}}^{K/K'}$ corresponding to the valley-current state are $\varphi_{\mathcal{B}}^{K/K'} = \pm C_{\mathcal{B}} sin\theta_{\boldsymbol{p}}$. Finally, this gives the valley current density $\boldsymbol{j}_v \equiv \boldsymbol{j}^K - \boldsymbol{j}^{K'} = 4\sigma_0 (el)^{-1} C_{\mathcal{B}} \hat{\boldsymbol{y}}$ along branch $\mathcal{B}$ with $\sigma_0 = \frac{1}{2} e^2 \nu_0 v_F^2 \tau$ to be the Drude conductivity for graphene per valley and per spin.

It remains to get an estimate for $C_{\mathcal{B}}$. For that we have to match the valley current on the $\mathcal{A}$ side of the interface line with that on the $\mathcal{B}$ side. To analyze the question in full detail, one has to solve the so-called diffuse emission problem for a given geometry (see, e.g., Refs. [23, 25]). We, however, limit ourselves to a qualitative discussion only. For a qualitative estimate, we use the distribution functions $\varphi_1^{K/K'}$ below the interface line, while above the line we take the distribution functions $\varphi_{\mathcal{B}}^{K/K'}$, i.e.,

$$\int_0^{\pi} sin\theta_{\boldsymbol{p}} \varphi_1^{K/K'} d\theta_{\boldsymbol{p}} \simeq \int_0^{2\pi} sin\theta_{\boldsymbol{p}} \varphi_{\mathcal{B}}^{K/K'} d\theta_{\boldsymbol{p}}. \tag{5.1}$$

Eventually, we get $C_{\mathcal{B}} \simeq 2B^{(2)}_{ph}/3\pi$ as an estimate for $C_{\mathcal{B}}$.

Now, let us discuss the mechanism of detecting the valley current. The main point here is that the valley current carriers inside the branch $\mathcal{B}$, in the process of collisions with phonons, generate a new term $\tilde{\varphi}_{\mathcal{B}}$ in the electron distribution function, with a nontrivial angular dependence. By solving the kinetic equation, we obtain (see Appendix C for details)

$$\tilde{\varphi}_{\mathcal{B}} = D^{(2)}_{ph} sin(2\theta_{\boldsymbol{p}}), \tag{5.2}$$

with $D^{(2)}_{ph} = (\Gamma^{(2)}_{e-ph}\tau)C_{\mathcal{B}}$. Because of the angular dependence of the distribution $\tilde{\varphi}_{\mathcal{B}}$, we expect to get a current flux injected into the side-directed branches chosen for recording.

In the discussed geometry, we suggest to measure electric currents flowing in the opposite directions (from left to right and from right to left) in two pairs of side branches $(\mathcal{C}, \tilde{\mathcal{C}})$ and $(\mathcal{D}, \tilde{\mathcal{D}})$, as shown in Fig. 5.1. Following the above discussion, the distribution function inside each of the branches, after a few collisions, acquires the Drude form. For example, inside branch $\mathcal{C}$ the function $\varphi_{\mathcal{C}}$ acquires the form $\varphi_{\mathcal{C}} = elE_{\mathcal{C}} cos(\theta_{\boldsymbol{p}} - \frac{\pi}{4})$. The combination $elE_{\mathcal{C}}$ could be estimated by matching the fluxes on both sides of interface 2. Similarly to Eq. (5.1), we get $elE_{\mathcal{C}} \simeq 2D^{(2)}_{ph}/3\pi$. Next, for branch $\mathcal{D}$, the injection yields the opposite sign, i.e., $E_{\mathcal{D}} = -E_{\mathcal{C}}$. Utilizing the chain of relations which connect $A_E$ with $B^{(2)}_{ph}$, $C_{\mathcal{B}}$, $D^{(2)}_{ph}$, and, finally, with $E_{\mathcal{C}}$ and $E_{\mathcal{D}}$, we can estimate the current density ratio for our design of the nonlocal transformer,

$$\frac{j_{\mathcal{C}}}{j_{\mathcal{A}}} = -\frac{j_{\mathcal{D}}}{j_{\mathcal{A}}} \simeq \frac{E_{\mathcal{C}}}{E} \simeq \frac{4}{9\pi^2}\left(\Gamma^{(2)}_{e-ph}\tau\right)^2. \tag{5.3}$$

## 6. DISCUSSION AND CONCLUSION*

In the remaining part of the thesis, we estimate the typical value of $j_{\mathcal{C}}/j_{\mathcal{A}}$. To do this, we extract the scattering time $\tau$ from the conductivity $\sigma_0$, by simply using the Drude formula, i.e., $\tau = \sigma_0/\frac{1}{2}e^2\nu_0 v_F^2$. Consequently, we find

$$\frac{j_{\mathcal{C}}}{j_{\mathcal{A}}} \simeq 0.6 \times 10^{-10} \left(\frac{\sigma_0(n)}{\sigma_q}\right)^2 \left(\frac{T}{T_{BG}(\tilde{n}=1)}\right)^2. \tag{6.1}$$

Here, the quantum conductivity $\sigma_q \equiv e^2/h$ is introduced as the unit of the conductivity. For metallic samples with a usual conductivity $\sigma_0(n)$ [4, 26], the current density ratio could be expected in the region $10^{-7} - 10^{-6}$. In the presence of a mismatch of the sample orientation, i.e., when $\eta \neq 0$, the discussed nonlocal effect survives. It is suppressed only by a geometric factor $cos^2(3\eta)$ [Appendix D].

Our consideration was limited to the case of degenerate electrons and the assumption that the intervalley scattering is negligible. Both assumptions limit the temperature from above. Still, because of a large difference between $v_s$ and $v_F$ in graphene, there remains a substantial interval of temperatures, $T_{BG} \ll T \ll \epsilon_F$, that could be addressed provided that $\tilde{n}$ is not so small.

Owing to the fact that the valley scattering length $l_v \gtrsim 1\ \mu m$, we expect that the current density ratios $j_{\mathcal{C}}/j_{\mathcal{A}}$ and $j_{\mathcal{D}}/j_{\mathcal{A}}$ could be measured through the geometry suggested by us in Fig. 5.1 with $1\ \mu m \gtrsim L_1, L_2 \gg l \simeq 10\ nm$. The strong inequality here is needed in order to reliably prevent the penetration of particles from region $\mathcal{A}$ straight into branches $(\mathcal{C}, \tilde{\mathcal{C}})$ and $(\mathcal{D}, \tilde{\mathcal{D}})$.

To conclude, we have argued that a valley current carried by quasiparticles could be generated and detected through a properly arranged geometric design. Our scheme relies on the fact that the term in the *el-ph* collision integral originating from a mixture of the scalar and vector gauge-field-like vertices has an opposite sign for the $K$ and $K'$ valleys. The effectiveness of the discussed mechanism grows with temperature by virtue of a greater *el-ph* collision rate at higher tempera-

*Reprinted with permission from "Valley current in graphene through electron-phonon interaction" by Ankang Liu and Alexander M. Finkel'stein, 2020. Phys. Rev. B, 101, 241401, Copyright 2020 by American Physical Society.

tures. In these respects, it differs entirely from the Berry curvature mechanism which works when the system is not far from the ground state, which has to be insulating. In short, our study provides an alternative approach to generate and detect the long-range propagating valley current in a pristine single- or double-layered graphene sample, which does not require the breaking of spatial inversion symmetry.

According to the estimates presented in this work, a current density ratio of the designed nonlocal transformer is small, but could be detected. The point is that the discussed mechanism does not have fragile elements, and is not sensitive to noise. Furthermore, since the quadruple character of the distribution is very specific, it can be checked by measuring currents in different branches. For example, if the information about the width of the branches, $w_{\mathcal{C}}$ and $w_{\mathcal{D}}$, is available, one may expect that $[(I_{\mathcal{C}}/w_{\mathcal{C}}) - (I_{\mathcal{D}}/w_{\mathcal{D}})] \gg [(I_{\mathcal{C}}/w_{\mathcal{C}}) + (I_{\mathcal{D}}/w_{\mathcal{D}})]$, and so on. In this way, one could exclude a parasitic signal that may come from a leakage from the region $\mathcal{A}$ to one of the branches. In current work, the generation and detection of the valley current was discussed in terms of the transport measurements. Alternatively, one can try to detect the valley polarization $\mu^K - \mu^{K'}$ which arises as a consequence of the injection of valley current inside branch $\mathcal{B}$ without introducing the side branches. Indeed, the valley polarization $\mu^K - \mu^{K'}$ in our scheme reaches the range of a few $meV$ at a distance of order $l_v$ from interface 1. Polarization of this scale can be detected in a pool at the end of branch $\mathcal{B}$ by the method considered in Ref. [27] or by magneto-oscillations (see, e.g., Ref. [28]).

From a fundamental point of view, the discussed mechanism, which holds generally for any honeycomb lattice system, demonstrates that the valley current can be of a kinetic origin, rather than be obligatorily related with the Berry curvature physics. Next, it opens a perspective to study the nontrivial aspects of the *el-ph* interaction, and the intervalley scattering rate at high temperatures. We expect this research could open up another unexplored possibility in the area of valleytronics.

REFERENCES


[1] J. R. Schaibley, H. Yu, G. Clark, P. Rivera, J. S. Ross, K. L. Seyler, W. Yao, and X. Xu, "Valleytronics in 2d materials," *Nature Reviews Materials*, vol. 1, no. 11, p. 16055, 2016.

[2] A. Liu and A. M. Finkel'stein, "Valley current in graphene through electron-phonon interaction," *Phys. Rev. B*, vol. 101, p. 241401, Jun 2020.

[3] A. H. Castro Neto, F. Guinea, N. M. R. Peres, K. S. Novoselov, and A. K. Geim, "The electronic properties of graphene," *Rev. Mod. Phys.*, vol. 81, pp. 109–162, Jan 2009.

[4] S. Das Sarma, S. Adam, E. H. Hwang, and E. Rossi, "Electronic transport in two-dimensional graphene," *Rev. Mod. Phys.*, vol. 83, pp. 407–470, May 2011.

[5] P. R. Wallace, "The band theory of graphite," *Phys. Rev.*, vol. 71, pp. 622–634, May 1947.

[6] D. Xiao, W. Yao, and Q. Niu, "Valley-contrasting physics in graphene: Magnetic moment and topological transport," *Phys. Rev. Lett.*, vol. 99, p. 236809, Dec 2007.

[7] D. Xiao, M.-C. Chang, and Q. Niu, "Berry phase effects on electronic properties," *Rev. Mod. Phys.*, vol. 82, pp. 1959–2007, Jul 2010.

[8] Y. D. Lensky, J. C. W. Song, P. Samutpraphoot, and L. S. Levitov, "Topological valley currents in gapped dirac materials," *Phys. Rev. Lett.*, vol. 114, p. 256601, Jun 2015.

[9] C. L. Kane and E. J. Mele, "Quantum spin hall effect in graphene," *Phys. Rev. Lett.*, vol. 95, p. 226801, Nov 2005.

[10] R. Gorbachev, J. Song, G. Yu, A. Kretinin, F. Withers, Y. Cao, A. Mishchenko, I. Grigorieva, K. Novoselov, L. Levitov, *et al.*, "Detecting topological currents in graphene superlattices," *Science*, vol. 346, no. 6208, pp. 448–451, 2014.

[11] Y. Shimazaki, M. Yamamoto, I. V. Borzenets, K. Watanabe, T. Taniguchi, and S. Tarucha, "Generation and detection of pure valley current by electrically induced berry curvature in bilayer graphene," *Nature Physics*, vol. 11, no. 12, p. 1032, 2015.

[12] M. Yamamoto, Y. Shimazaki, I. V. Borzenets, and S. Tarucha, "Valley hall effect in two-dimensional hexagonal lattices," *Journal of the Physical Society of Japan*, vol. 84, no. 12, p. 121006, 2015.

[13] L. M. Woods and G. D. Mahan, "Electron-phonon effects in graphene and armchair (10,10) single-wall carbon nanotubes," *Phys. Rev. B*, vol. 61, pp. 10651–10663, Apr 2000.

[14] H. Suzuura and T. Ando, "Phonons and electron-phonon scattering in carbon nanotubes," *Phys. Rev. B*, vol. 65, p. 235412, May 2002.

[15] J. L. Mañes, "Symmetry-based approach to electron-phonon interactions in graphene," *Phys. Rev. B*, vol. 76, p. 045430, Jul 2007.

[16] E. Mariani and F. von Oppen, "Temperature-dependent resistivity of suspended graphene," *Phys. Rev. B*, vol. 82, p. 195403, Nov 2010.

[17] W. Chen and A. A. Clerk, "Electron-phonon mediated heat flow in disordered graphene," *Phys. Rev. B*, vol. 86, p. 125443, Sep 2012.

[18] R. E. Prange and L. P. Kadanoff, "Transport theory for electron-phonon interactions in metals," *Phys. Rev.*, vol. 134, pp. A566–A580, May 1964.

[19] A. Kamenev, *Field theory of non-equilibrium systems*. Cambridge University Press, 2011.

[20] J. Rammer and H. Smith, "Quantum field-theoretical methods in transport theory of metals," *Rev. Mod. Phys.*, vol. 58, pp. 323–359, Apr 1986.

[21] L. Landau, E. Lifshitz, and L. Pitaevskij, *Course of theoretical physics. vol. 10: Physical kinetics*. Oxford, 1981.

[22] W. Knap, C. Skierbiszewski, A. Zduniak, E. Litwin-Staszewska, D. Bertho, F. Kobbi, J. L. Robert, G. E. Pikus, F. G. Pikus, S. V. Iordanskii, V. Mosser, K. Zekentes, and Y. B. Lyanda-Geller, "Weak antilocalization and spin precession in quantum wells," *Phys. Rev. B*, vol. 53, pp. 3912–3924, Feb 1996.

[23] A. Shekhter, M. Khodas, and A. M. Finkel'stein, "Diffuse emission in the presence of an inhomogeneous spin-orbit interaction for the purpose of spin filtration," *Phys. Rev. B*, vol. 71, p. 125114, Mar 2005.

[24] M. Khodas, *Transport Properties of Two Dimensional Systems in the Presence of Disorder and Spin-Orbit Interaction*. PhD thesis, Weizmann Institute of Science, 2005 (Unpublished).

[25] P. M. Morse and H. Feshbach, *Methods of theoretical physics*. McGraw-Hill, New York, 1953.

[26] Y.-W. Tan, Y. Zhang, K. Bolotin, Y. Zhao, S. Adam, E. H. Hwang, S. Das Sarma, H. L. Stormer, and P. Kim, "Measurement of scattering rate and minimum conductivity in graphene," *Phys. Rev. Lett.*, vol. 99, p. 246803, Dec 2007.

[27] T. O. Wehling, A. Huber, A. I. Lichtenstein, and M. I. Katsnelson, "Probing of valley polarization in graphene via optical second-harmonic generation," *Phys. Rev. B*, vol. 91, p. 041404(R), Jan 2015.

[28] A. A. Abrikosov, *Fundamentals of the Theory of Metals*. Courier Dover Publications, 2017.

[29] A. A. Abrikosov, L. P. Gorkov, and I. E. Dzyaloshinski, *Methods of quantum field theory in statistical physics*. Courier Corporation, 2012.

[30] M. Schütt, P. M. Ostrovsky, I. V. Gornyi, and A. D. Mirlin, "Coulomb interaction in graphene: Relaxation rates and transport," *Phys. Rev. B*, vol. 83, p. 155441, Apr 2011.

[31] K. Kechedzhi, O. Kashuba, and V. I. Fal'ko, "Quantum kinetic equation and universal conductance fluctuations in graphene," *Phys. Rev. B*, vol. 77, p. 193403, May 2008.

[32] E. McCann and M. Koshino, "The electronic properties of bilayer graphene," *Reports on Progress in Physics*, vol. 76, p. 056503, apr 2013.

[33] H. Ochoa, E. V. Castro, M. I. Katsnelson, and F. Guinea, "Temperature-dependent resistivity in bilayer graphene due to flexural phonons," *Phys. Rev. B*, vol. 83, p. 235416, Jun 2011.

# APPENDIX A

## DERIVATION OF QUANTUM KINETIC EQUATION*

Here we present the details of the derivation for the quantum kinetic equation in graphene. We concentrate on electrons in the $K$-valley. To begin with, we start with the left-right subtracted Dyson equation for the Keldysh component [20]

$$(G_0^{-1} - \Sigma^R) \otimes G^K - G^K \otimes (G_0^{-1} - \Sigma^A) + G^R \otimes \Sigma^K - \Sigma^K \otimes G^A = 0. \tag{A.1}$$

Here $\otimes$ means the convolution in the space-time coordinates. We then transform Eq. (A.1) to the mixed Wigner coordinate according to the gradient expansion rule and keep only the leading terms that contribute to the quantum kinetic equation. We get

$$i\Big(\partial_t G^K + i[\boldsymbol{\sigma}\cdot\boldsymbol{p}, G^K]_- + \frac{1}{2}v_F[\boldsymbol{\sigma}, \nabla_{\boldsymbol{r}} G^K]_+\Big) - [Re(\Sigma^R), G^K]_- - i[Im(\Sigma^R), G^K]_+ \\ + G^R\Sigma^K - \Sigma^K G^A = 0. \tag{A.2}$$

The subscript $\mp$ here in $[A, B]_\mp$ means commutator and anti-commutator of A and B, respectively. We also used the fact that $G_0^{-1} = (\epsilon + \epsilon_F)\mathbb{1} - v_F\boldsymbol{\sigma}\cdot\boldsymbol{p}$ in the mixed coordinate, where $\mathbb{1}$ is the $2\times 2$ identity matrix. In Eq. (A.2), terms that contain the gradient of the self-energy are neglected, because they only renormalize the parameters in the kinetic part of the equation, while our attention is on the collision integral.

In Eq. (A.2), the retarded, advanced, and the Keldysh components of the self-energy arising as

*Reprinted with permission from "Valley current in graphene through electron-phonon interaction" by Ankang Liu and Alexander M. Finkel'stein, 2020. Phys. Rev. B, 101, 241401, Copyright 2020 by American Physical Society.

the result of the *el-ph* interaction are as follows [19, 20]:

$$\Sigma^{R/A}(\epsilon,\boldsymbol{p}) = \frac{i}{2}\int\frac{d\omega}{2\pi}\int\frac{d^2\boldsymbol{q}}{(2\pi)^2}\Big\{M_{-\boldsymbol{q}}G^{R/A}(\epsilon+\omega,\boldsymbol{p}+\boldsymbol{q})M_{\boldsymbol{q}}D^{K}(\omega,\boldsymbol{q}) + M_{-\boldsymbol{q}}G^{K}(\epsilon+\omega,\boldsymbol{p}+\boldsymbol{q})M_{\boldsymbol{q}}D^{A/R}(\omega,\boldsymbol{q})\Big\}; \tag{A.3}$$

$$\Sigma^{K}(\epsilon,\boldsymbol{p}) = \frac{i}{2}\int\frac{d\omega}{2\pi}\int\frac{d^2\boldsymbol{q}}{(2\pi)^2}\Big\{M_{-\boldsymbol{q}}G^{K}(\epsilon+\omega,\boldsymbol{p}+\boldsymbol{q})M_{\boldsymbol{q}}D^{K}(\omega,\boldsymbol{q}) - M_{-\boldsymbol{q}}\big[G^{R}(\epsilon+\omega,\boldsymbol{p}+\boldsymbol{q}) - G^{A}(\epsilon+\omega,\boldsymbol{p}+\boldsymbol{q})\big]M_{\boldsymbol{q}}\big[D^{R}(\omega,\boldsymbol{q}) - D^{A}(\omega,\boldsymbol{q})\big]\Big\}. \tag{A.4}$$

Here $M_{\boldsymbol{q}}$ is the *el-ph* interaction vertex, which is a $2\times 2$ matrix that has been presented in the main text. Only the one-loop diagram has been considered.

Now, we apply the quasi-classical approximation by taking advantage of the fact that the self-energies (A.3) and (A.4) are slow functions of the variable $\xi_{\boldsymbol{p}} = v_F p - \epsilon_F$. After making the integration "$\frac{1}{\pi}\int d\xi_{\boldsymbol{p}}\cdots$" on both sides of Eq. (A.2), it becomes

$$\partial_t g^K + ip_F[\boldsymbol{\sigma}\cdot\boldsymbol{n}_{\boldsymbol{p}}, g^K]_- + \frac{1}{2}v_F[\boldsymbol{\sigma},\nabla_{\boldsymbol{r}}g^K]_+ + i[Re(\Sigma^R), g^K]_- - [Im(\Sigma^R), g^K]_+ - i(g^R\Sigma^K - \Sigma^K g^A) = 0. \tag{A.5}$$

Here, the electron momentum $\boldsymbol{p}$ was placed on the Fermi surface. The self-energies in Eq. (A.5) are

$$\begin{aligned}\Sigma^{R/A}(\epsilon,\boldsymbol{n}_{\boldsymbol{p}}) &\equiv \Sigma^{R/A}(\epsilon,\boldsymbol{p}=p_F\boldsymbol{n}_{\boldsymbol{p}})\\ &\simeq \frac{\nu_0}{4}\int d\epsilon'\int\frac{d\theta_{\boldsymbol{p}'}}{2\pi}\alpha(q)\Big\{(g_1\mathbb{1}+g_2\boldsymbol{d}\cdot\boldsymbol{\sigma})(g^{R/A})'(g_1\mathbb{1}+g_2\boldsymbol{d}\cdot\boldsymbol{\sigma})D^K\\ &\quad + (g_1\mathbb{1}+g_2\boldsymbol{d}\cdot\boldsymbol{\sigma})(g^K)'(g_1\mathbb{1}+g_2\boldsymbol{d}\cdot\boldsymbol{\sigma})D^{A/R}\Big\};\end{aligned} \tag{A.6}$$

$$\Sigma^K(\epsilon, \boldsymbol{n_p}) \equiv \Sigma^K(\epsilon, \boldsymbol{p} = p_F \boldsymbol{n_p})$$
$$\simeq \frac{\nu_0}{4} \int d\epsilon' \int \frac{d\theta_{\boldsymbol{p}'}}{2\pi} \alpha(q) \Big\{ (g_1 \mathbb{1} + g_2 \boldsymbol{d} \cdot \boldsymbol{\sigma})(g^K)'(g_1 \mathbb{1} + g_2 \boldsymbol{d} \cdot \boldsymbol{\sigma}) D^K$$
$$- (g_1 \mathbb{1} + g_2 \boldsymbol{d} \cdot \boldsymbol{\sigma}) \big[ (g^R)' - (g^A)' \big] (g_1 \mathbb{1} + g_2 \boldsymbol{d} \cdot \boldsymbol{\sigma}) \big[ D^R - D^A \big] \Big\}. \tag{A.7}$$

In the above expressions we have used short notations to indicate the arguments in Green's functions. Namely, $(g^{K/R/A})' = g^{K/R/A}(\epsilon', \boldsymbol{n_{p'}})$ and $D^{K/R/A} = D^{K/R/A}(\epsilon' - \epsilon, p_F(\boldsymbol{n_{p'}} - \boldsymbol{n_p}))$. Here, we also take $\eta = 0$, and $\nu_0$, $\alpha(q)$, $\boldsymbol{d}$ and $\boldsymbol{q}$ are defined as in the main text. The quasi-classical Green's function $g^{R/A} = \pm \hat{P}_+ + \delta g^{R/A}$, where the main term $\hat{P}_+ = \frac{1}{2}(\mathbb{1} + \boldsymbol{n_p} \cdot \boldsymbol{\sigma})$ is the "+ chirality" projection operator. The correction term $\delta g^{R/A}$, which is negligible, will be considered in the next section (Appendix B).

Next, we substitute the approximation $g^{R/A} \simeq \pm \hat{P}_+$, the ansatz $g^K = h(g^R - g^A) \simeq 2h\hat{P}_+$, and the general expression

$$\Sigma^{K/R/A} = \Sigma_a^{K/R/A} \mathbb{1} + \Sigma_b^{K/R/A} \boldsymbol{n_p} \cdot \boldsymbol{\sigma} + \Sigma_c^{K/R/A} (\hat{z} \times \boldsymbol{n_p}) \cdot \boldsymbol{\sigma} \tag{A.8}$$

in Eq. (A.5). Finally, after taking trace on both sides of Eq. (A.5), one could obtain

$$\partial_t h + v_F \boldsymbol{n_p} \cdot \nabla_{\boldsymbol{r}} h - 2h Im(\Sigma_a^R + \Sigma_b^R) - i(\Sigma_a^K + \Sigma_b^K) = 0 \tag{A.9}$$

by noticing that $ip_F[\boldsymbol{\sigma} \cdot \boldsymbol{n_p}, g^K]_- = 0$ and that the term $i[Re(\Sigma^R), g^K]_-$ is traceless.

In order to get the Boltzmann-like quantum kinetic equation, we have to find $Im(\Sigma_{a/b}^R)$ and $\Sigma_{a/b}^K$. With the use of Eqs. (A.6)&(A.7), and with the relation $D^K = N(D^R - D^A)$, one could straightforwardly obtain

$$2iIm(\Sigma_a^R) = \frac{1}{2} Tr(\Sigma^R - \Sigma^A)$$
$$\simeq \frac{\nu_0}{4} \int d\epsilon' \int \frac{d\theta_{\boldsymbol{p}'}}{2\pi} \alpha(q) [g_1^2 + 2g_1 g_2 (\boldsymbol{n_{p'}} \cdot \boldsymbol{d}) + g_2^2](N - h')[D^R(\omega, \boldsymbol{q}) - D^A(\omega, \boldsymbol{q})], \tag{A.10}$$

and

$$2iIm(\Sigma_b^R) = \frac{1}{2}Tr[(\boldsymbol{n_p}\cdot\boldsymbol{\sigma})(\Sigma^R-\Sigma^A)]$$
$$\simeq \frac{\nu_0}{4}\int d\epsilon' \int \frac{d\theta_{\boldsymbol{p'}}}{2\pi}\alpha(q)\{g_1^2(\boldsymbol{n_p}\cdot\boldsymbol{n_{p'}})+2g_1g_2(\boldsymbol{n_p}\cdot\boldsymbol{d})+g_2^2[-(\boldsymbol{n_p}\cdot\boldsymbol{n_{p'}})$$
$$+2(\boldsymbol{n_p}\cdot\boldsymbol{d})(\boldsymbol{n_{p'}}\cdot\boldsymbol{d})]\}(N-h')[D^R(\omega,\boldsymbol{q})-D^A(\omega,\boldsymbol{q})]. \tag{A.11}$$

Similarly, we also find

$$\Sigma_a^K = \frac{1}{2}Tr(\Sigma^K)$$
$$\simeq \frac{\nu_0}{4}\int d\epsilon' \int \frac{d\theta_{\boldsymbol{p'}}}{2\pi}\alpha(q)[g_1^2+2g_1g_2(\boldsymbol{n_{p'}}\cdot\boldsymbol{d})+g_2^2](N\cdot h-1)[D^R(\omega,\boldsymbol{q})-D^A(\omega,\boldsymbol{q})], \tag{A.12}$$

and

$$\Sigma_b^K = \frac{1}{2}Tr[(\boldsymbol{n_p}\cdot\boldsymbol{\sigma})\Sigma^K]$$
$$\simeq \frac{\nu_0}{4}\int d\epsilon' \int \frac{d\theta_{\boldsymbol{p'}}}{2\pi}\alpha(q)\{g_1^2(\boldsymbol{n_p}\cdot\boldsymbol{n_{p'}})+2g_1g_2(\boldsymbol{n_p}\cdot\boldsymbol{d})+g_2^2[-(\boldsymbol{n_p}\cdot\boldsymbol{n_{p'}})+2(\boldsymbol{n_p}\cdot\boldsymbol{d})(\boldsymbol{n_{p'}}\cdot\boldsymbol{d})]\}$$
$$\times(N\cdot h-1)[D^R(\omega,\boldsymbol{q})-D^A(\omega,\boldsymbol{q})]. \tag{A.13}$$

In the expressions above, $h\equiv h(\epsilon,\boldsymbol{n_p})$, $h'\equiv h(\epsilon',\boldsymbol{n_{p'}})$ and $N\equiv N(\omega,\boldsymbol{q})=1+2n(\omega,\boldsymbol{q})$. Again, $\omega$ and $\boldsymbol{q}$ here should be understood as $\omega=\epsilon'-\epsilon$ and $\boldsymbol{q}=p_F(\boldsymbol{n_{p'}}-\boldsymbol{n_p})$. The above results, together with $D^R(\omega,\boldsymbol{q})-D^A(\omega,\boldsymbol{q})=-2\pi i[\delta(\omega-\omega_{\boldsymbol{q}})-\delta(\omega+\omega_{\boldsymbol{q}})]$, and Eq. (A.9), immediately lead to the equation

$$\partial_t h+\boldsymbol{v}_F\cdot\nabla_{\boldsymbol{r}}h=\frac{\pi\nu_0}{2}\int d\epsilon'\int\frac{d\theta_{\boldsymbol{p'}}}{2\pi}\alpha(q)\big\{g_1^2(1+\boldsymbol{n_p}\cdot\boldsymbol{n_{p'}})+2g_1g_2(\boldsymbol{n_p}+\boldsymbol{n_{p'}})\cdot\boldsymbol{d}$$
$$+g_2^2\big[(1-\boldsymbol{n_p}\cdot\boldsymbol{n_{p'}})+2(\boldsymbol{n_p}\cdot\boldsymbol{d})(\boldsymbol{n_{p'}}\cdot\boldsymbol{d})\big]\big\}[h'h+N(h'-h)-1](\delta_+-\delta_-). \tag{A.14}$$

Here $\boldsymbol{v}_F \equiv v_F \boldsymbol{n}_{\boldsymbol{p}}$. Eventually, by rewriting $h = 1 - 2f$ and $N = 1 + 2n$, we obtain the desired equation

$$\partial_t f + \boldsymbol{v}_F \cdot \nabla_{\boldsymbol{r}} f = I_{e-ph}(f, n) \tag{A.15}$$

with $I_{e-ph}(f, n)$ to be the *el-ph* collision integral:

$$I_{e-ph}(f,n) = \pi\nu_0 \int d\epsilon' \int \frac{d\theta_{\boldsymbol{p}'}}{2\pi} \alpha(q) \big\{ g_1^2 (1 + \boldsymbol{n}_{\boldsymbol{p}} \cdot \boldsymbol{n}_{\boldsymbol{p}'}) + 2 g_1 g_2 (\boldsymbol{n}_{\boldsymbol{p}} + \boldsymbol{n}_{\boldsymbol{p}'}) \cdot \boldsymbol{d} + g_2^2 \big[ (1 - \boldsymbol{n}_{\boldsymbol{p}} \cdot \boldsymbol{n}_{\boldsymbol{p}'}) + 2 (\boldsymbol{n}_{\boldsymbol{p}} \cdot \boldsymbol{d})(\boldsymbol{n}_{\boldsymbol{p}'} \cdot \boldsymbol{d}) \big] \big\} \big[ f'(1-f)(1+n) - f(1-f')n \big] (\delta_+ - \delta_-). \tag{A.16}$$

Eq. (A.15) is just the Boltzmann-like quantum kinetic equation. In particular, the mixed $g_1 g_2$-term in Eq. (A.16) is the non-trivial *el-ph* collision integral $I^v_{e-ph}(f, n)$ that we discuss in the main text. Note that the angular dependence of the *el-ph* scattering given by the curly brackets in Eq. (A.16) coincides with that obtained in Ref. [16] for the transition probability induced by phonons. Furthermore, the expression for the electric current density is given by [20]:

$$\begin{aligned} \boldsymbol{j} &= -\frac{1}{2} \nu_0 Tr \Big\{ \int d\epsilon \int \frac{d\theta_{\boldsymbol{p}}}{2\pi} \big[ e \hat{\boldsymbol{v}} g^K(\epsilon, \boldsymbol{n}_{\boldsymbol{p}}) \big] \Big\} \\ &= 2e\nu_0 \int d\epsilon \int \frac{d\theta_{\boldsymbol{p}}}{2\pi} \big[ \boldsymbol{v}_F f(\epsilon, \boldsymbol{n}_{\boldsymbol{p}}) \big]. \end{aligned} \tag{A.17}$$

Here $\hat{\boldsymbol{v}}$ is the velocity operator $\partial_{\boldsymbol{p}} H_{\boldsymbol{p}} = v_F(\sigma_x, \sigma_y)$. We see that the matrix structure of $\hat{\boldsymbol{v}}$ and $g^K$ after tracing out leads to a conventional expression for the current density through the Fermi velocity $\boldsymbol{v}_F$ and quasi-classical distribution function $f$. The coefficient in front of the integral takes into consideration the pseudo-spin as well as the real spin degrees of freedom.

## APPENDIX B

## SMALLNESS OF $\delta g^{R/A}$ *

In this section, we consider correction $\delta g^{R/A}$ induced by the *el-ph* interaction, following the ideas of section 21 in Ref. [29]. We only check the case of the single layered graphene here, while the bilayer one is similar. From Dyson equation, we have $G^R = (G_0^{-1} - \Sigma^R)^{-1}$, where $G_0$ is the free electron propagator and $G_0^{-1} = (\epsilon + \epsilon_F)\mathbb{1} - v_F \boldsymbol{\sigma}\cdot\boldsymbol{p}$. In principle, the self-energy $\Sigma^R$ is a function of $G^{K/R/A}$ and one has to solve $G$ and $\Sigma$ simultaneously. Here, we assume that a self-consistent approximation for the quasi-classical Green's function is $g^R = \hat{P}_+ + \delta g^R \simeq \hat{P}_+$. Under this assumption, the quasi-classically approximated self-energy is [see Eq. (A.6)]

$$\begin{aligned}\Sigma^R(\epsilon, \boldsymbol{n_p}) &\equiv \Sigma^R(\epsilon, \boldsymbol{p} = p_F \boldsymbol{n_p}) \\ &\simeq \frac{\nu_0}{4}\int d\epsilon' \int \frac{d\theta_{\boldsymbol{p}'}}{2\pi}\alpha(q)\Big\{(g_1\mathbb{1} + g_2 \boldsymbol{d}\cdot\boldsymbol{\sigma})(\hat{P}_+)'(g_1\mathbb{1} + g_2\boldsymbol{d}\cdot\boldsymbol{\sigma})D^K \\ &+ (g_1\mathbb{1} + g_2\boldsymbol{d}\cdot\boldsymbol{\sigma})[2h'(\hat{P}_+)'](g_1\mathbb{1} + g_2\boldsymbol{d}\cdot\boldsymbol{\sigma})D^A\Big\} \\ &= \Sigma_a^R\mathbb{1} + \Sigma_b^R \boldsymbol{n_p}\cdot\boldsymbol{\sigma} + \Sigma_c^R(\hat{z}\times\boldsymbol{n_p})\cdot\boldsymbol{\sigma}. \end{aligned} \tag{B.1}$$

Then, we have

$$\begin{aligned} G^R &= \{G_0^{-1} - [\Sigma_a^R\mathbb{1} + \Sigma_b^R\boldsymbol{n_p}\cdot\boldsymbol{\sigma} + \Sigma_c^R(\hat{z}\times\boldsymbol{n_p})\cdot\boldsymbol{\sigma}]\}^{-1} \\ &= G^{R(0)} + G^{R(0)}[\Sigma_c^R(\hat{z}\times\boldsymbol{n_p})\cdot\boldsymbol{\sigma}]G^{R(0)} + \cdots . \end{aligned} \tag{B.2}$$

*Reprinted with permission from "Valley current in graphene through electron-phonon interaction" by Ankang Liu and Alexander M. Finkel'stein, 2020. Phys. Rev. B, 101, 241401, Copyright 2020 by American Physical Society.

Here, we define $G^{R(0)} = \{G_0^{-1} - [\Sigma_a^R \mathbb{1} + \Sigma_b^R \boldsymbol{n_p} \cdot \boldsymbol{\sigma}]\}^{-1} = \hat{P}_+ G_+^{R(0)} + \hat{P}_- G_-^{R(0)}$, where $G_\pm^{R(0)}$ is [30]

$$G_\pm^{R(0)} = \frac{Z}{(\epsilon + \epsilon_F) \mp v_F^* p - iZIm(\Sigma_\pm^R)} \tag{B.3}$$

with

$$Z = [1 - \frac{Re(\Sigma_a^R)}{\epsilon + \epsilon_F}]^{-1},\ v_F^* = v_F Z[1 + \frac{Re(\Sigma_b^R)}{v_F p}],\ \Sigma_\pm^R = \Sigma_a^R \pm \Sigma_b^R. \tag{B.4}$$

In metals, usually, the *el-ph* self-energy renormalizes the Fermi velocity, yielding an effect of the order 1. Here it is not the case. The reason lies in the smallness of the Fermi-momentum. For the metallic graphene, $p_F \ll a^{-1}$, where $a$ is a typical atomic length. Since $\nu_0 \propto p_F$ the effect is small, we have $Z \approx 1$ and $v_F^* \approx v_F$.

In order to find the quasi-classical Green's function, we make $\xi_{\boldsymbol{p}}$-integration on both sides of Eq. (B.2) around the Fermi surface [31]. This gives

$$g^R = \frac{i}{\pi} \int d\xi_{\boldsymbol{p}} G^R = \hat{P}_+ + \delta g^R. \tag{B.5}$$

Here, $\hat{P}_+$ comes from the $\hat{P}_+$-term in $G^{R(0)}$. Correction $\delta g^R$ originates from $\Sigma_c^R(\hat{z} \times \boldsymbol{n_p}) \cdot \boldsymbol{\sigma}$. If the self-energy is small enough, $\delta g^R$ is determined by the finite limits of integration over $\xi_{\boldsymbol{p}}$, and could be neglected.

Hence, one may ask for justification of smallness of $\Sigma_c^R$ as well as the possibility of neglecting its dependence on $\xi_{\boldsymbol{p}}$. First of all, at relatively high temperature, $T \gg T_{BG}$, phonons with large momentum are excited. Hence, more local phonons are involved. For the short-range physics, the *el-ph* scattering is less dependent on $\xi_{\boldsymbol{p}}$. Therefore, it is safe to neglect the $\xi_{\boldsymbol{p}}$-dependence of $\Sigma_c^R$ for this temperature regime. Moreover, for the metallic graphene one could find that $\Sigma_c^R$ is strongly bounded by an upper limit, $|\Sigma_c^R| \ll T_{BG}$, at high temperatures, and thus only gives a negligible $\delta g^R$ in this situation. However, there is no guarantee for the low temperature regime $T \ll T_{BG}$.

We check for this case specifically.

From Eq. (A.3), we have

$$\begin{aligned}\Sigma_c^R &= \frac{1}{2}Tr\{[(\hat{z}\times\boldsymbol{n_p})\cdot\boldsymbol{\sigma}]\Sigma^R\}\\ &\simeq \frac{i}{2}\int\frac{d\omega}{2\pi}\int\frac{d^2\boldsymbol{q}}{(2\pi)^2}\alpha(q)[g_1g_2\big((\hat{z}\times\boldsymbol{n_p})\cdot\boldsymbol{d}\big)+g_2^2(\boldsymbol{n_{p+q}}\cdot\boldsymbol{d})\big((\hat{z}\times\boldsymbol{n_p})\cdot\boldsymbol{d}\big)]\\ &\times[G_+^{R(0)}(\epsilon+\omega,\boldsymbol{p}+\boldsymbol{q})D^K(\omega,\boldsymbol{q})+G_+^{K(0)}(\epsilon+\omega,\boldsymbol{p}+\boldsymbol{q})D^A(\omega,\boldsymbol{q})]. \qquad \text{(B.6)}\end{aligned}$$

To proceed further, we split the self-energy $\Sigma_c^R$ into two parts, i.e., $\Sigma_c^R = (\Sigma_c^R)_1 + (\Sigma_c^R)_2$, where $(\Sigma_c^R)_1$ and $(\Sigma_c^R)_2$ are the terms which are proportional to $g_1g_2$ and $g_2^2$ in Eq. (B.6), respectively. Then, (for simplification) without considering the screening effect of $g_1$, we find

$$\begin{aligned}|\delta g^R| &\sim \int d\xi_{\boldsymbol{p}}G_+^{R(0)}\Big[iIm[(\Sigma_c^R)_1]\Big]G_+^{R(0)}\\ &\simeq sin(3\theta_{\boldsymbol{p}})\big(\frac{\pi}{2}\big)\int\frac{d\xi_{\boldsymbol{p}}d\omega qdqd\theta}{(2\pi)^3}\alpha(q)g_1g_2cos(2\theta)[coth(\frac{\omega}{2T})-tanh(\frac{\epsilon+\omega}{2T})]\big(\frac{1}{\epsilon-\xi_{\boldsymbol{p}}-iIm(\Sigma_+^R)}\big)^2\\ &\times\{\frac{1}{\epsilon+\omega-\xi_{\boldsymbol{p}}-v_Fqcos(\theta)-iIm(\Sigma_+^{R'})}-\frac{1}{\epsilon+\omega-\xi_{\boldsymbol{p}}-v_Fqcos(\theta)+iIm(\Sigma_+^{R'})}\}\\ &\times[\delta(\omega-\omega_{\boldsymbol{q}})-\delta(\omega+\omega_{\boldsymbol{q}})]\\ &\sim\big(\frac{v_s}{v_F}\big)\begin{cases}T/\omega_c, & |\epsilon|\ll T\\ |\epsilon|/\omega_c, & T\ll|\epsilon|\end{cases}. \qquad \text{(B.7)}\end{aligned}$$

Here $\theta=\theta_{\boldsymbol{p}}-\theta_{\boldsymbol{q}}$, $\Sigma_+^R=\Sigma_+^R(\epsilon)$ and $\Sigma_+^{R'}=\Sigma_+^R(\epsilon+\omega)$. In the calculation above, we have assumed both electrons and phonons under the thermal equilibrium, approximated $\xi_{\boldsymbol{p+q}}\simeq\xi_{\boldsymbol{p}}+v_Fqcos(\theta)$, and also neglected the $\xi_{\boldsymbol{p}}$-dependence of $\Sigma_+^R$. In Eq. (B.7), $\omega_c$ is a characteristic energy, which we find to be $\omega_c=\frac{\rho v_F v_s^3}{g_1g_2}$. Taking $\rho\approx 7.6\times10^{-7}\ kg\cdot m^{-2}$, $v_F\approx10^6\ m/s$ and $v_s\approx2.1\times10^4\ m/s$, we estimate $\omega_c$ to be 1.1 $\sim$ 1.6 eV. When the screening effect of $g_1$ is considered, we replace $g_1$ by $g_1^{sc}(q)=g_1\frac{q}{q+\kappa_{TF}}\simeq g_1\frac{q}{\kappa_{TF}}$, where $\kappa_{TF}$ is the Thomas-Fermi wavevector. In graphene, $\kappa_{TF}$ is approximately equal to $8p_F$ [16], where $p_F$ is the Fermi momentum. Following the same

calculation, we obtain

$$|\delta g^R| \sim \left(\frac{v_s}{v_F}\right) \begin{cases} \frac{T^2}{\omega_c(v_s\kappa_{TF})}, & |\epsilon| \ll T \\ \frac{\epsilon^2}{\omega_c(v_s\kappa_{TF})}, & T \ll |\epsilon| \end{cases}. \tag{B.8}$$

At reasonable temperatures, and not too high frequencies, we have $|\delta g^R| \ll \frac{v_s}{v_F} \ll 1$. Another contribution to $\delta g^R$ which comes from $(\Sigma_c^R)_2$ could be checked similarly. It is also suppressed by the small factor $\frac{v_s}{v_F}$. Finally, the smallness of $\delta g^R$ has been verified for all situations considered in this research.

To conclude, we are limited only by the applicability of the method of quasi-classics itself, rather than complications induced by the *el-ph* interaction. Therefore, system should be not too close to the neutrality point, and temperature should not exceed $\epsilon_F$.

## APPENDIX C

## SOLUTION OF THE QUANTUM KINETIC EQUATION*

In this section, we present detailed discussion of the solution of the quantum kinetic equation which leads to the valley-contrasting dynamics. We start with Eqs. (A.15)&(A.16). As shown in the main text, we simply need to solve Eq. (4.3) iteratively. Since the *el-ph* term yields only a correction (albeit a non-trivial one), one could easily extract as the main term the Drude-kind solution $\varphi_0 = A_E cos\theta_{\boldsymbol{p}}$ with $A_E = v_F eE\tau = elE$, where $l \equiv v_F\tau$ is the mean free path length. The main term $\varphi_0$ here describes the conventional transport properties of graphene which gives electric current density $\boldsymbol{j}_D = 4\sigma_0\boldsymbol{E}$, when the both valleys are considered. In the following, the non-trivial correction functions $\varphi_1^{K/K'}$ will be found in two asymptotic temperature regimes, namely, $T \ll T_{BG}$ and $T \gg T_{BG}$.

### C.1 Low Temperatures ($T \ll T_{BG}$)

In the low temperature regime, $Q_T \equiv (\frac{T}{v_s}) \ll p_F,\ \kappa_{TF}$. This means a small scattering angle $\theta = \theta_{\boldsymbol{p}'} - \theta_{\boldsymbol{p}} \ll 1$, and we could also use the approximated after-screening coupling constant $g_1^{sc} \simeq g_1\frac{q}{\kappa_{TF}}$. As the result, we get

$$[I^v_{e-ph}]^{K/K'}(\varphi_0) = \mp\Gamma_{e-ph}(-\frac{\partial f_0}{\partial\epsilon})A_E[cos(2\theta_{\boldsymbol{p}}) - 2cos(4\theta_{\boldsymbol{p}})] \tag{C.1}$$

with

$$\Gamma_{e-ph} \simeq \frac{3840\zeta(5)}{\pi}\left(\frac{g_1 g_2 p_F^2}{\rho v_s v_F}\right)\left(\frac{p_F}{\kappa_{TF}}\right)\left(\frac{T}{T_{BG}}\right)^5. \tag{C.2}$$

Here $\zeta(s)$ is the Riemann zeta function, and $\zeta(5) \approx 1.037$. Consequently, $\varphi_1^{K/K'} = \mp B_{ph}[cos(2\theta_{\boldsymbol{p}}) - 2cos(4\theta_{\boldsymbol{p}})]$ with $B_{ph} = (\Gamma_{e-ph}\tau)A_E$.

*Reprinted with permission from "Valley current in graphene through electron-phonon interaction" by Ankang Liu and Alexander M. Finkel'stein, 2020. Phys. Rev. B, 101, 241401, Copyright 2020 by American Physical Society.

### C.2 High Temperatures ($T \gg T_{BG}$)

For the high temperatures, the approximation we could use is $n_0(\omega) = (e^{\omega/T} - 1)^{-1} \simeq \frac{T}{\omega}$. In addition, for the screened coupling constant we have $g_1^{sc}(q) = g_1 \frac{q}{q+\kappa_{TF}}$. With this in mind, we get

$$[I^v_{e-ph}]^{K/K'}(\varphi_0) = \mp[\Gamma^{(2)}_{e-ph}(-\frac{\partial f_0}{\partial \epsilon})A_E cos(2\theta_{\boldsymbol{p}}) + \Gamma^{(4)}_{e-ph}(-\frac{\partial f_0}{\partial \epsilon})A_E cos(4\theta_{\boldsymbol{p}})] \tag{C.3}$$

with

$$\Gamma^{(2)}_{e-ph} \simeq \frac{1}{\pi}\left(\frac{g_1 g_2 p_F^2}{\rho v_s v_F}\right)\left(\frac{T}{T_{BG}}\right)\left[G\left(\frac{\kappa_{TF}}{2p_F}\right) - F\left(\frac{\kappa_{TF}}{2p_F}\right)\right] \tag{C.4}$$

and

$$\Gamma^{(4)}_{e-ph} \simeq \frac{1}{\pi}\left(\frac{g_1 g_2 p_F^2}{\rho v_s v_F}\right)\left(\frac{T}{T_{BG}}\right)\left[-G\left(\frac{\kappa_{TF}}{2p_F}\right) - F\left(\frac{\kappa_{TF}}{2p_F}\right)\right]. \tag{C.5}$$

Here, functions $F$ and $G$ are associated with the angular integration in the *el-ph* collision integral. They are

$$F(x) = \int d\theta \left(\frac{sin|\frac{\theta}{2}|}{sin|\frac{\theta}{2}| + x}\right) cos(\frac{\theta}{2}) cos(\frac{3\theta}{2}) \left[1 - cos(\theta)\right] \tag{C.6}$$

and

$$G(x) = \int d\theta \left(\frac{sin|\frac{\theta}{2}|}{sin|\frac{\theta}{2}| + x}\right) cos(\frac{\theta}{2}) sin(\frac{3\theta}{2}) sin(\theta). \tag{C.7}$$

For $\kappa_{TF} \simeq 8p_F$, we find $F(4) \approx -0.282$ and $G(4) \approx 0.169$. In this case, we get $\varphi_1^{K/K'} = \mp[B^{(2)}_{ph} cos(2\theta_{\boldsymbol{p}}) + B^{(4)}_{ph} cos(4\theta_{\boldsymbol{p}})]$, where $B^{(2/4)}_{ph} = (\Gamma^{(2/4)}_{e-ph}\tau)A_E$.

Now, we briefly justify the statement $I_0(\varphi) \gg [I^v_{e-ph}]^{K/K'}(\varphi)$, which is the argument we have used for perturbative solving the kinetic equation. Since we have $I_0(\varphi) \propto (\frac{1}{\tau})(\delta f)$ and

$[I^{v}_{e-ph}]^{K/K'}(\varphi) \propto (\Gamma_{e-ph})(\delta f)$, the equivalent description of this inequality is $\Gamma_{e-ph}\tau \ll 1$. For low temperatures, $T \ll T_{BG}$, we find $\Gamma_{e-ph}\tau \simeq 3.86 \times 10^{-2} \times \sqrt{\tilde{n}} \times (\frac{\sigma_0}{\sigma_q}) \times (\frac{T}{T_{BG}})^5$ , while for $T \gg T_{BG}$ we have $\Gamma^{(2)}_{e-ph}\tau \simeq 3.49 \times 10^{-5} \times \sqrt{\tilde{n}} \times (\frac{\sigma_0}{\sigma_q}) \times (\frac{T}{T_{BG}})$ and $\Gamma^{(4)}_{e-ph}\tau \simeq 8.79 \times 10^{-6} \times \sqrt{\tilde{n}} \times (\frac{\sigma_0}{\sigma_q}) \times (\frac{T}{T_{BG}})$. Here, for the combination determining the value of the *el-ph* interaction we take $\frac{g_1 g_2 p_F^2}{\rho v_s v_F} \simeq 1.42 \times 10^{-5} \times \tilde{n}$ eV, while the transport time $\tau$ is estimated as $\tau = \sigma_0/\frac{1}{2}e^2\nu_0 v_F^2 \simeq 1.13 \times 10^{-2} \times (\frac{1}{\sqrt{\tilde{n}}}) \times (\frac{\sigma_0}{\sigma_q})\ ps$. Recall that $1\ ps^{-1} = 7.64\ K$, while 1 eV $= 1.16 \times 10^4\ K$. Obviously, the perturbative approach to the solution of the kinetic equation could be applied for a typical graphene sample in all temperature regimes we considered in this work.

### C.3 Discussion

In order to complete the full description of the valley-dependent dynamics, we have to consider also the situation where the external electric field is along an arbitrary direction which has an angle $\theta_{\boldsymbol{E}}$ with respect to the zigzag direction of the lattice. In our current coordinate system, i.e., $\eta = 0$, we have $\boldsymbol{E} = E(cos\theta_{\boldsymbol{E}}, sin\theta_{\boldsymbol{E}})$. Then, the electric field enters the kinetic equation as $eEcos(\theta_{\boldsymbol{p}} - \theta_{\boldsymbol{E}})$, and $\varphi_0$ simply changes to $\varphi_0 = A_E cos(\theta_{\boldsymbol{p}} - \theta_{\boldsymbol{E}})$. As a result, for $\varphi_1^{K/K'}$ one gets the following changes: $cos(2\theta_{\boldsymbol{p}}) \to cos(2\theta_{\boldsymbol{p}} + \theta_{\boldsymbol{E}})$ and $cos(4\theta_{\boldsymbol{p}}) \to cos(4\theta_{\boldsymbol{p}} - \theta_{\boldsymbol{E}})$. Alternatively, one may rotate the coordinate system to $\hat{x} \parallel \boldsymbol{E}$. From this point of view, we just need to set $\eta = \theta_{\boldsymbol{E}}$, and use a modified expression for $\boldsymbol{d} = \big(cos(2\theta_{\boldsymbol{q}} + 3\theta_{\boldsymbol{E}}), -sin(2\theta_{\boldsymbol{q}} + 3\theta_{\boldsymbol{E}})\big)$ in Eq. (4.2). Eventually, these two considerations give the same solution.

The results here are very useful when discussing the detection of the valley current. For example, in our designed geometry, the valley current propagating along the branch $\mathcal{B}$ is carried by the valley-dependent distributions $\varphi_{\mathcal{B}}^{K/K'} = \pm C_{\mathcal{B}} sin\theta_{\boldsymbol{p}}$. To detect this valley current, we again use the non-trivial *el-ph* collision integral. Namely, by solving the equation $I_0(\tilde{\varphi}_{\mathcal{B}}) + [I^{v}_{e-ph}]^{K/K'}(\varphi_{\mathcal{B}}^{K/K'}) = 0$, we get a valley-*independent* distribution $\tilde{\varphi}_{\mathcal{B}}$. To obtain the magnitude of the effect, we can interpret the function $\sim sin(\theta_{\boldsymbol{p}})$ as a solution in response to the fake electric field directed along the $y$-direction, i.e., $\theta_{\boldsymbol{E}} = \frac{\pi}{2}$. Then, by utilizing our results for an arbitrarily directed $\boldsymbol{E}$, we immediately find the solution $\tilde{\varphi}_{\mathcal{B}}$ is $\tilde{\varphi}_{\mathcal{B}} = D_{ph}[sin(2\theta_{\boldsymbol{p}}) + 2sin(4\theta_{\boldsymbol{p}})]$ with $D_{ph} = (\Gamma_{e-ph}\tau)C_{\mathcal{B}}$ for $T \ll T_{BG}$, or $\tilde{\varphi}_{\mathcal{B}} = [D^{(2)}_{ph} sin(2\theta_{\boldsymbol{p}}) - D^{(4)}_{ph} sin(4\theta_{\boldsymbol{p}})]$ with $D^{(2/4)}_{ph} = (\Gamma^{(2/4)}_{e-ph}\tau)C_{\mathcal{B}}$ for $T \gg T_{BG}$.

Collecting everything together, we are ready to discuss the non-local current density ratio $j_{\mathcal{C}}/j_{\mathcal{A}}$ in two different temperature regimes. We estimate the coefficients $C_{\mathcal{B}}$ and $E_{\mathcal{C}}$ by matching the fluxes at the Interface 1 and 2 similar to Eq. (5.1) with the inclusion of both 2nd and 4th harmonics. As for $T \ll T_{BG}$, we find

$$\frac{j_{\mathcal{C}}}{j_{\mathcal{A}}} \simeq \frac{4}{15\pi^2}\left(\Gamma_{e-ph}\tau\right)^2 \simeq 4.02\times 10^{-5}\times\tilde{n}\times\left(\frac{\sigma_0}{\sigma_q}\right)^2\left(\frac{T}{T_{BG}(\tilde{n})}\right)^{10}. \tag{C.8}$$

In the above expression, we use the same notations as in the main text. As an example, let us consider $\tilde{n}=1$ and $T=0.3\,T_{BG}$. Then, the large power factor in the above expression yields $6\times 10^{-6}$. One can see that for usual, at this range of concentrations ($\sim 10^{12}\ cm^{-2}$), conductivity $\sigma_0 \gtrsim 10\sigma_q$ [4, 26], the current density ratio could be expected in the region $\sim 10^{-8}$. For the high temperature regime $T \gg T_{BG}$, we get

$$\begin{aligned}\frac{j_{\mathcal{C}}}{j_{\mathcal{A}}} &\simeq \frac{4}{9\pi^2}\left(1+\frac{\Gamma^{(4)}_{e-ph}}{5\Gamma^{(2)}_{e-ph}}\right)\left(\Gamma^{(2)}_{e-ph}\tau\right)^2 \\ &\approx \frac{4}{9\pi^2}\left(\Gamma^{(2)}_{e-ph}\tau\right)^2 \simeq 5.49\times 10^{-11}\times\tilde{n}\times\left(\frac{\sigma_0}{\sigma_q}\right)^2\left(\frac{T}{T_{BG}(\tilde{n})}\right)^2.\end{aligned} \tag{C.9}$$

Here, in the second line of Eq. (C.9), we dropped the small term $\Gamma^{(4)}_{e-ph}/5\Gamma^{(2)}_{e-ph} \simeq 0.05 \ll 1$. This justifies our claim made in the main text that the 4th harmonic contributes much less than the 2nd harmonic does to the non-local signal at high temperatures. If we take $\tilde{n}=1$ and $T=10\,T_{BG}$, the current density ratio could be expected in the region $10^{-7}\sim 10^{-6}$.

As expected, the non-local effect increases with temperature due to the higher *el-ph* collision rate. Notice that there is a big mismatch at $(\frac{T}{T_{BG}(\tilde{n})})=1$ between the low- and high-temperature estimates obtained for $j_{\mathcal{C}}/j_{\mathcal{A}}$. This is not surprising in view of a very strong dependence on the factor $(\frac{T}{T_{BG}(\tilde{n})})$ obtained in Eq. (C.8) for low temperatures. The two estimates match each other at $T\approx 0.185\,T_{BG}\approx \frac{1}{2\pi}\,T_{BG}$.

So far, in our discussions, we have neglected the inter-valley scattering. However, if $L_1, L_2 > l_v$, one has to consider the inter-valley scattering inside the branch $\mathcal{B}$. This will add a decay factor

$e^{-\frac{L_1+L_2}{l_v}}$ (or $e^{-\frac{L_1}{l_v}}$) to our expression for $j_{\mathcal{C}}/j_{\mathcal{A}}$ (or $j_{\mathcal{D}}/j_{\mathcal{A}}$) in Eq. (5.3).

One more remark about the character of the elastic scattering. Recall that we considered only the system in which the scattering in $I_0(\varphi)$ is short-ranged. Then, the relaxation time is the same for all harmonics. However, in the opposite limit, when the scattering is dominated by the *smooth* scattering potentials, the relaxation times are $\tau$, $\tau/4$ and $\tau/16$ for the 1st, 2nd and 4th harmonic, respectively [22]. As a consequence, in a real system, which has a combination of both short-ranged and smooth scattering potentials, the non-local current density ratio $j_{\mathcal{C}}/j_{\mathcal{A}}$ could be a few times smaller, than in our previous estimations.

## APPENDIX D

## THE EFFECT OF THE MISMATCH ANGLE*

In our discussion, we assumed that the region $\mathcal{A}$ is along the $x$-direction, which in our system of coordinates is along the zigzag direction of the honeycomb lattice. In other words, the mismatch angle was ignored so far, $\eta = 0$. In this section, we discuss the effects induced by a non-zero $\eta$. First of all, with $\eta \neq 0$, we find that the valley-dependent solution in region $\mathcal{A}$ becomes

$$\varphi_1^{K/K'} = \begin{cases} \mp B_{ph}[cos(2\theta_{\boldsymbol{p}} + 3\eta) - 2cos(4\theta_{\boldsymbol{p}} + 3\eta)], & T \ll T_{BG} \\ \mp[B_{ph}^{(2)} cos(2\theta_{\boldsymbol{p}} + 3\eta) + B_{ph}^{(4)} cos(4\theta_{\boldsymbol{p}} + 3\eta)], & T \gg T_{BG} \end{cases}. \tag{D.1}$$

This solution has been obtained through two steps. We start with our results found in the previous part for an arbitrary electric field with $\theta_{\boldsymbol{E}} = \eta$. Then we rotate the whole system with an angle $\eta$ by re-defining $\theta_{\boldsymbol{p}}$, i.e., $\theta_{\boldsymbol{p}} - \eta \to \theta_{\boldsymbol{p}}$. The changes here lead to the modification of the coefficient, $C_{\mathcal{B}} \to cos(3\eta) C_{\mathcal{B}}$.

Next, the valley-*independent* solution $\tilde{\varphi}_{\mathcal{B}}$ in branch $\mathcal{B}$ changes as well,

$$\tilde{\varphi}_{\mathcal{B}} = \begin{cases} D_{ph}[sin(2\theta_{\boldsymbol{p}} + 3\eta) + 2sin(4\theta_{\boldsymbol{p}} + 3\eta)], & T \ll T_{BG} \\ [D_{ph}^{(2)} sin(2\theta_{\boldsymbol{p}} + 3\eta) - D_{ph}^{(4)} sin(4\theta_{\boldsymbol{p}} + 3\eta)], & T \gg T_{BG} \end{cases}. \tag{D.2}$$

By matching the fluxes at the Interface 2 and 3, we obtain the coefficients $E_{\mathcal{C}}$ and $E_{\mathcal{D}}$ which determine the magnitude of the non-local current densities. For the low temperatures, $T \ll T_{BG}$, we get

$$\begin{aligned} elE_{\mathcal{C}} &\simeq \left( \frac{2}{3\pi} cos(3\eta) + \frac{4}{15\pi} sin(3\eta) \right) D_{ph}; \\ elE_{\mathcal{D}} &\simeq -\left( \frac{2}{3\pi} cos(3\eta) - \frac{4}{15\pi} sin(3\eta) \right) D_{ph}. \end{aligned} \tag{D.3}$$

*Reprinted with permission from "Valley current in graphene through electron-phonon interaction" by Ankang Liu and Alexander M. Finkel'stein, 2020. Phys. Rev. B, 101, 241401, Copyright 2020 by American Physical Society.

As for $T \gg T_{BG}$, we find

$$elE_{\mathcal{C}} \simeq \left( \frac{2}{3\pi} cos(3\eta) D_{ph}^{(2)} - \frac{2}{15\pi} sin(3\eta) D_{ph}^{(4)} \right);$$
$$elE_{\mathcal{D}} \simeq - \left( \frac{2}{3\pi} cos(3\eta) D_{ph}^{(2)} + \frac{2}{15\pi} sin(3\eta) D_{ph}^{(4)} \right). \tag{D.4}$$

We see that there appears a minor difference between the absolute values of $E_{\mathcal{C}}$ and $E_{\mathcal{D}}$ for a small $\eta$, which is caused by the 4th harmonics. Note that, for the high temperature regime, this difference is negligible, because $\Gamma_{e-ph}^{(4)}/5\Gamma_{e-ph}^{(2)} \ll 1$. By neglecting this difference, we get

$$\frac{j_{\mathcal{C}}}{j_{\mathcal{A}}} \approx -\frac{j_{\mathcal{D}}}{j_{\mathcal{A}}} \approx \frac{4}{9\pi^2} cos^2(3\eta) \left( \Gamma_{e-ph}^{(2)} \tau \right)^2 \tag{D.5}$$

at the high temperatures. To conclude, in the presence of mismatch, the discussed non-local effect survives. At relatively high temperatures, it is suppressed only by a geometric factor $cos^2(3\eta)$. For a small mis-orientation of the measurement scheme with respect to the zigzag lattice direction, i.e., when $\eta \ll 1$, the modification is negligible. (Recall that orientation of the scheme is defined with respect to the direction of the branch $\mathcal{A}$, which is denoted to be the $x$-direction.) However, there are “unfortunate" angles, e.g., $\pi/6$, when the whole valley current effect disappears.

## APPENDIX E

## QUANTUM KINETIC EQUATION AND VALLEY-DEPENDENT DYNAMICS FOR DOUBLE LAYERED GRAPHENE*

The derivation of the quantum kinetic equation for the double layered graphene is given by making direct comparison with the single layered one. There are several differences between the two cases. First, the effective Hamiltonians for free electrons are rather different. For the bilayer graphene with $AB$-stacking, the effective low energy Hamiltonian in $K$-valley under the basis of $A_1/B_2$ sublattices is $H_e^{bi} = \sum_{\boldsymbol{p}} \Psi_{\boldsymbol{p}}^\dagger H_{\boldsymbol{p}}^{bi} \Psi_{\boldsymbol{p}}$, where $H_{\boldsymbol{p}}^{bi}$ is [32, 33]

$$H_{\boldsymbol{p}}^{bi} = \frac{1}{2m} \begin{pmatrix} 0 & (p_x - ip_y)^2 \\ (p_x + ip_y)^2 & 0 \end{pmatrix} - \epsilon_F \mathbb{1}_{2\times 2}. \tag{E.1}$$

The effective mass $m$ originates from the inter-layer hopping, $2m = \frac{t_\perp}{v_F^2}$, where the inter-layer hopping $t_\perp \simeq 0.3$ eV. Since this effective Hamiltonian is valid only for low energies, so we require $\epsilon_F \lesssim 0.1 t_\perp$. At the upper limit, let it be $\epsilon_F = \frac{p_F^2}{2m} = 0.1 t_\perp$, we still have $v_F^{bi} \gg v_s$; here $v_F^{bi} = \frac{p_F}{m} \simeq 0.66 v_F$. This justifies the validity of the quasi-classical approximation. As a result, in the case of bilayer graphene, we have to replace $\boldsymbol{n_p}$ in the previous derivation by $\boldsymbol{n}_{\boldsymbol{p}}^{bi} = (cos(2\theta_{\boldsymbol{p}}), sin(2\theta_{\boldsymbol{p}}))$.

The second difference is the *el-ph* interaction vertices. For bilayer graphene, we have $H_{e-ph}^{bi} = \sum_{\boldsymbol{p},\boldsymbol{q}} \Psi_{\boldsymbol{p}+\boldsymbol{q}}^\dagger M_{\boldsymbol{p}+\boldsymbol{q},\boldsymbol{p}}^{bi} \Psi_{\boldsymbol{p}} A_{\boldsymbol{q}}$ with a matrix $M_{\boldsymbol{p}+\boldsymbol{q},\boldsymbol{p}}^{bi}$ [33]

$$M_{\boldsymbol{p}+\boldsymbol{q},\boldsymbol{p}}^{bi} = |\boldsymbol{q}| \sqrt{\frac{1}{2\rho^{bi}\omega_{\boldsymbol{q}}}} \begin{pmatrix} g_1^{bi} & g_2^{bi} C \\ g_2^{bi} C^* & g_1^{bi} \end{pmatrix}, \tag{E.2}$$

where the off-diagonal matrix elements $C = [\frac{p}{p_F} e^{-i\theta_{\boldsymbol{p}}} + \frac{p'}{p_F} e^{-i\theta_{\boldsymbol{p}'}}] e^{i(2\theta_{\boldsymbol{q}}+3\eta)} \Big|_{\boldsymbol{p}'=\boldsymbol{p}+\boldsymbol{q}}$. For the coupling constants in bilayer graphene, we have $g_1^{bi} = g_1$ and $g_2^{bi} = \frac{v_F^{bi}}{2v_F} g_2$.

*Reprinted with permission from "Valley current in graphene through electron-phonon interaction" by Ankang Liu and Alexander M. Finkel'stein, 2020. Phys. Rev. B, 101, 241401, Copyright 2020 by American Physical Society.

Additionally, because of the quadratic dispersion of the electron spectrum in bilayer graphene, we need to replace $\xi_{\boldsymbol{p}}$ by $\xi^{bi}_{\boldsymbol{p}} = \frac{p^2}{2m} - \epsilon_F$. Furthermore, the density of state per valley and per spin on the Fermi surface in this case is changed to be $\nu_0^{bi} = \frac{m}{2\pi}$. Hence, when the screening effect in bilayer graphene is considered, $(g_1^{bi})^{sc}(q) = g_1^{bi}\frac{q}{q+\kappa_{TF}^{bi}}$ where $\kappa_{TF}^{bi} \simeq 4\frac{t_\perp}{v_F}$.

Under the quasi-classical approximation, $M^{bi}_{\boldsymbol{p+q},\boldsymbol{p}}$ becomes

$$M^{bi}_{\boldsymbol{p+q},\boldsymbol{p}} \simeq \tilde{M}^{bi}_{\boldsymbol{n_{p'}},\boldsymbol{n_p}}(\boldsymbol{q}) = |\boldsymbol{q}|\sqrt{\frac{1}{2\rho^{bi}\omega_{\boldsymbol{q}}}}\begin{pmatrix} g_1^{bi} & g_2^{bi}\tilde{C} \\ g_2^{bi}\tilde{C}^* & g_1^{bi}\end{pmatrix}, \tag{E.3}$$

where now $\tilde{C}$ depends only on angles, $\tilde{C} = [e^{-i\theta_{\boldsymbol{p}}} + e^{-i\theta_{\boldsymbol{p'}}}]e^{i(2\theta_{\boldsymbol{q}}+3\eta)}$. This leads to the replacement of $\boldsymbol{d} = (cos(2\theta_{\boldsymbol{q}}), -sin(2\theta_{\boldsymbol{q}}))$ by $\boldsymbol{d}^{bi} = \big(cos(2\theta_{\boldsymbol{q}} - \theta_{\boldsymbol{p}}) + cos(2\theta_{\boldsymbol{q}} - \theta_{\boldsymbol{p'}}), -sin(2\theta_{\boldsymbol{q}} - \theta_{\boldsymbol{p}}) - sin(2\theta_{\boldsymbol{q}} - \theta_{\boldsymbol{p'}})\big)$ in the course of the derivation. We take $\eta = 0$ here as well.

Everything else remains the same as in the derivation for the single layered graphene. Finally, our Boltzmann-like quantum kinetic equation for the quasi-classical distribution function $f$ in the double layered graphene is

$$\partial_t f + \boldsymbol{v}_F^{bi} \cdot \nabla_{\boldsymbol{r}} f = I^{bi}_{e-ph}(f, n) \tag{E.4}$$

with $I^{bi}_{e-ph}(f,n)$ to be

$$\begin{aligned} I^{bi}_{e-ph}(f,n) = \pi\nu_0^{bi}\int d\epsilon' \int \frac{d\theta_{\boldsymbol{p'}}}{2\pi}\alpha^{bi}(q)\big\{(g_1^{bi})^2(1+\boldsymbol{n}\cdot\boldsymbol{n}') + 2g_1^{bi}g_2^{bi}(\boldsymbol{n}+\boldsymbol{n}')\cdot\boldsymbol{d}^{bi} \\ + (g_2^{bi})^2\big[(\boldsymbol{d}^{bi})^2(1-\boldsymbol{n}\cdot\boldsymbol{n}') + 2(\boldsymbol{n}\cdot\boldsymbol{d}^{bi})(\boldsymbol{n}'\cdot\boldsymbol{d}^{bi})\big]\big\}\big[f'(1-f)(1+n) - f(1-f')n\big](\delta_+ - \delta_-). \end{aligned} \tag{E.5}$$

In the expressions above, $\boldsymbol{n}$, $\boldsymbol{n}'$ are $\boldsymbol{n}^{bi}_{\boldsymbol{p}}$ and $\boldsymbol{n}^{bi}_{\boldsymbol{p'}}$; $\boldsymbol{v}_F^{bi} \equiv v_F^{bi}\boldsymbol{n}_{\boldsymbol{p}}$ and $\alpha^{bi}(q) = \frac{q^2}{2\rho^{bi}\omega_{\boldsymbol{q}}}$ with $\rho^{bi}$ to be the mass density for bilayer graphene. Other notations are the same as in Eq. (A.16).

The velocity operator acquires the form $\hat{\boldsymbol{v}}^{bi} = \partial_{\boldsymbol{p}}H^{bi}_{\boldsymbol{p}}\Big|_{\boldsymbol{p}=\boldsymbol{p}_F} = v_F^{bi}\big(cos(\theta_{\boldsymbol{p}})\sigma_x + sin(\theta_{\boldsymbol{p}})\sigma_y, -sin(\theta_{\boldsymbol{p}})\sigma_x + cos(\theta_{\boldsymbol{p}})\sigma_y\big)$. With the ansatz $g^K = (1-2f)(g^R - g^A) = (1-2f)(\mathbb{1} + \boldsymbol{n}^{bi}_{\boldsymbol{p}}\cdot\boldsymbol{\sigma})$, we obtain again

the conventional expression for the electric current density, $\boldsymbol{j} = 2e\nu_0^{bi}\int d\epsilon \int \frac{d\theta_{\boldsymbol{p}}}{2\pi}\left[\boldsymbol{v}_F^{bi} f(\epsilon, \boldsymbol{n}_{\boldsymbol{p}})\right]$.

In terms of the transformation from $K$ to $K'$-valley, we have the free electron Hamiltonian and the *el-ph* interaction vertex in $K'$-valley become [15]

$$(H_{\boldsymbol{p}}^{bi})^{K'} = \frac{1}{2m}\begin{pmatrix} 0 & (p_x + ip_y)^2 \\ (p_x - ip_y)^2 & 0 \end{pmatrix} - \epsilon_F \mathbb{1}_{2\times 2} \tag{E.6}$$

and

$$(M_{\boldsymbol{p}+\boldsymbol{q},\boldsymbol{p}}^{bi})^{K'} = |\boldsymbol{q}|\sqrt{\frac{1}{2\rho\omega_{\boldsymbol{q}}}}\begin{pmatrix} g_1^{bi} & -g_2^{bi}C^* \\ -g_2^{bi}C & g_1^{bi} \end{pmatrix}. \tag{E.7}$$

As a result, we observe that, for the double layered (like for the single layered) graphene, the $g_1^{bi}g_2^{bi}$-term in the *el-ph* collision integral Eq. (E.5) becomes opposite in $K'$-valley when Eqs. (E.6)&(E.7) are compared with Eqs. (E.1)&(E.2). All discussions on the valley-dependent dynamics, e.g., the generation of a valley-contrasting quadruple angular distribution, that we did for single layer graphene, also work for bilayer graphene.